TÉCNICO LISBOA

Ethylene Dichloride Cracker Modelling and State Estimation

Susana Broeiro Bento

Thesis to obtain the Master of Science Degree in

Chemical Engineering

Supervisors

Sreekumar Maroor (PSE)

Prof. Henrique Matos (IST)

Examination Committee

President: Profª Teresa Duarte

Supervisor: Prof. Henrique Matos

Members of the Committee: Prof. Rui Filipe

November 2017

Look wide, beyond your immediate surroundings and limits,
And you see things in their right proportion.
Look above the level of things around you
And see a higher aim and possibility to your work.

Lord Robert Baden-Powell

Acknowledgements

First of all, I would like to thank my supervisors from IST, Prof. Henrique Matos, and from PSE, Sreekumar Maroor and Stepan Spatenka.

To Prof. Henrique Matos I would like to thank for the great opportunity provided for doing my master thesis at PSE and all the support and feedback of my work.

To Sreekumar Maroor, for the guidance, availability and the share of knowledge. I also would like to thank Stepan Spatenka for all the help he gave me during the past six months and to Filipe Calado for helping me with state estimation implementation.

I could not miss thanking Renato Wong for all the help he gave me for the development of my work, his commitment, and his generosity towards me, whether in time spent or in piece of advice given.

I will always be thankful to all the Portuguese community in PSE, for making London feel like home. Special thanks to André, Artur, Renato and Tom for sharing their home with us and providing shelter when we needed it.

To all the friends I made in PSE, particularly Lilya and Piero, who made this experience much richer and unforgettable.

To Joana, Luis and Ricardo, my housemates, who shared with me this once in a lifetime experience, for have given me so many good memories.

Thanks to all the friends I found during my years at IST, for all of the support and for making everything much easier.

Finally, I would like to thank my amazing big family, my parents, brothers and sister, for always being there for me and encourage me to always go further.

Resumo

O cloreto de vinilo (VCM) é um dos mais importantes produtos químicos de base e é usado essencialmente para produzir cloreto de polivinilo (PVC). O VCM é produzido através da pirólise de dicloroetano (EDC). A formação de produtos secundários é inevitável, tornando importante a adequada modelação do processo em vista à sua optimização.

Procedeu-se então à configuração de um modelo da pirólise do EDC, com base no modelo da fornalha desenvolvido pela PSE. Este modelo inclui o *cracking tube*, constituído pelos modelos cinéticos de *cracking* e formação de coque, bem como o modelo responsável pela interpolação do perfil de temperaturas. O mecanismo cinético implementado foi estudado por Choi et. Al [1] e consiste em 108 reações, envolvendo 47 componentes.

Os resultados do modelo foram comparados com os resultados de outro modelo, que usa um mecanismo cinético ajustado a dados reais de uma unidade. Os resultados para os principais componentes apresentam desvios de 1.4 - 1.9%.

Foi realizada uma simulação dinâmica, em que os resultados de queda de pressão e caudais de saída de EDC e VCM ao longo do ciclo foram comparados com dados de uma unidade. Foi implementada a técnica de *Sate Estimation,* que permitiu uma melhoria nos resultados.

Finalmente, foi estudada a possibilidade de redução do esquema cinético. Permitindo um desvio de 0.1% em relação aos resultados originais, verificou-se que 48 reações poderiam ser excluídas, sem comprometer o desempenho do modelo. Deveriam ser feitos mais testes, considerando um maior número de impurezas à entrada da fornalha, para validar esta possível redução.

Palavras-chave: Modelação, VCM, pirólise, mecanismo radicalar, gPROMS

Abstract

Vinyl Chloride monomer (VCM) is one of the most important commodity chemicals and it is produced mainly by the cracking of ethylene dichloride (EDC). By-products formation is inevitable, creating several inefficiencies, and accurate model of the process is essential for its optimization

In the present work, an EDC cracker model was set-up using the furnace model from gPROMS ProcessBuilder, developed by PSE. The cracking kinetic mechanism implemented consists of 108 reversible reactions and 47 components, as reported by Choi et al. [1]

The model predictions were compared to predictions from another model which used a cracking kinetic model tuned to plant data. The deviations for the main components were in the range of 1.4-1.9%. The deviations for impurities were more significant.

A dynamic simulation of a cycle was carried out. The predictions of pressure drop, VCM flow rate and EDC flow rate over the cycle were compared to plant data. Subsequently, state estimations were performed to assess the feasibility of improving the model predictions and the initial results are positive.

Finally, a study regarding the possibility of reducing the cracking kinetic scheme was initiated. Allowing a deviation of 0.1% from the original results, it was verified that 48 reactions could be excluded without compromising the model accuracy. More tests considering other impurities in the furnace feed should be done to further validate this possible kinetic scheme reduction.

Keywords: modelling, VCM, cracking, radical mechanism, state estimation, gPROMS

Contents

List of Tables

List of Figures

Glossary

CFD	Computational Fluid Dynamics
CIP	Coil Inlet Pressure
COP	Coil Outlet Pressure
CIT	Coil Inlet Temperature
COT	Coil Outlet Temperature
EDC	Ethylene dichloride or dichloroethane
EDCM1	Ethylene dichloride cracker model 1 – Model developed by PSE previously to this work to model a specific industrial unit
EDCM2	Ethylene dichloride cracker model 2 – Model developed in this work
FO	Foreign Object
HCl	Hydrogen Chloride
HTC	High-Temperature Chlorination
LSKM	Large Scale Kinetic Mechanism
LTC	Low-Temperature Chlorination
NC	Number of components
TCE	1,1,2-trichloroethane
VCM	Vinyl Chloride Monomer

Nomenclature

A	Pre-exponential factor
b	Temperature exponent
C	Molar concentration
C_p	Heat capacity
CRR_{adj}	Coking reaction rate adjustment parameter
ΔH_f	Formation enthalpy
ΔH^o	Change of standard enthalpy
ΔS^o	Change of standard entropy
E_a	Activation energy
f	Forward
G	Mass flux
i	Component
j	Reaction
K_c	Equilibrium constant
k	Kinetic constant
M_w	Molecular weight
n	Reaction order
P	Pressure
R	Gas constant
r	Reaction rate
T	Temperature
T_{ref}	Reference temperature
w	Mass fraction
z	Axial position

1. Introduction

The commercial significance of the vinyl chloride monomer (VCM) can be highlighted by the production of polyvinyl chloride (PVC), the world's second most abundant plastic. Approximately 96% of the VCM production is used for the production of PVC.

PVC is used in the most diverse sectors, ranging from healthcare to construction and electronics. It is present, for example, in blood bags and tubing, wire and cable insulation or windshield system components. [2]

Currently, vinyl chloride is mainly produced through the thermal cracking of ethylene dichloride (EDC). This process begins with chlorination of ethylene to ethylene dichloride, followed by its dehydrochlorination to VCM. The thermal cracking of EDC to VCM takes place in a pyrolysis furnace at temperatures around 500^{o}C. [3]

In principle, the complex thermal cracking of EDC is considered to proceed via free-radical reactions. Rigorous reaction mechanisms have been studied and improved by various researchers. [4] Ranzi et al. introduced a reaction kinetic scheme with more than 200 elementary reactions with more than 40 molecular and radical species. Borsa et al. [3] developed the most complex cracking kinetic mechanism for EDC pyrolysis, including 135 compounds and radical species and more than 800 reactions. Choi et al. [1] established a mechanism that involves 108 reversible reactions and 47 molecular/radical species. The addition of carbon tetrachloride as promoter was first investigated by Choi et al. [1] Schirmeister et al. [5] simplified the foregoing EDC pyrolysis mechanism aiming the data accuracy and expenditure optimization for model adjustment. A total of 31 reactions, 18 compounds, and 8 radical species were used to describe all relevant products, intermediates, and byproducts. [4]

A typical EDC conversion would be between 50 and 60%, to limit by-product formation and obtain selectivity to VCM around 99%. [3]

Even though it is possible to achieve high yields, the formation of by-products is inevitable, causing significant inefficiencies in the process. Coke formation is an important reason for concern since its deposition inside the reactor coils demands periodical shutdowns of the unit. Besides coke, there are other gas phase impurities such as chloroprene and butadiene that cause downstream difficulties in distillation columns.

Having this in consideration, it is important to accurately model the process aiming the model-based process optimization. In the past, the manufacture of vinyl chloride monomers (VCM) raised concerns regarding hazard, safety and pollution. Therefore, the VCM technology was among the first to profit from improvements suggested by process simulation. As a result, the modern VCM plants are today among the cleanest and safest in the chemical process industries. [6]

1.1 Motivation

This work aims to configure a model of an industrial EDC cracker that accurately describes the real process and apply state estimation using real plant data.

The model will be set-up using the already existing furnace model libraries within gPROMS ProcessBuilder, developed by Process Systems Enterprise Ltd.

The model will be used with real plant data to test the feasibility of applying state estimation on this system.

In the end, the possibility of a kinetic scheme reduction will also be explored, aiming a reduction in the size and complexity of the model.

2. Background

2.1 Overview of VCM and PVC Market

Vinyl chloride monomer (VCM) is one of the world's most important commodity chemicals, and it is used mainly for the production of polyvinyl chloride (PVC) [7].

PVC is an ubiquitous plastic very often selected for construction, piping, and many other sectors due to the polymer properties, including its light weight, chemical resistance, and versatility. [8]

VCM is among the top twenty largest petrochemicals regarding world production, and its manufacturing technology has been improving from the standpoint of safety, environment, quality, and scale of production. [9]

The chart presented in Figure 1 shows the world consumption of vinyl chloride monomer.

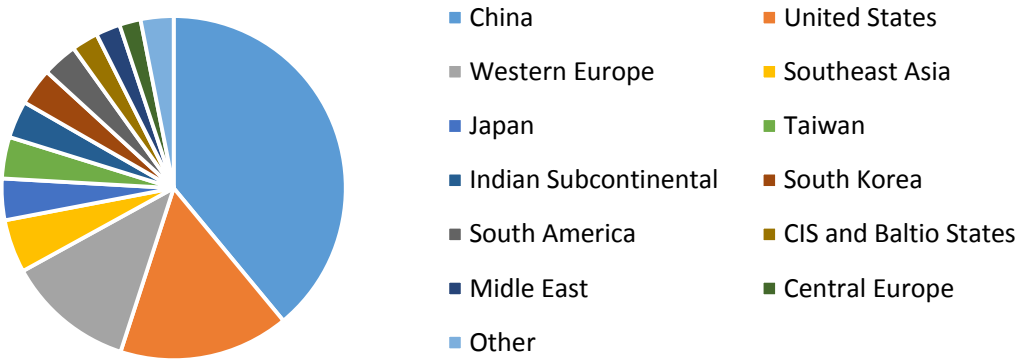

Figure 1 – World Consumption of vinyl chloride monomer (2015) [9]

China is the largest player in the VCM market, with nearly half of the total world capacity and about 38–39% of total global production and consumption in 2015. The United States follows as the second-largest player worldwide and maintains a low-production-cost position in chlorine and ethylene raw materials. The movement towards lower natural gas and feedstock costs for the vinyl chain in North America, via shale gas, is solidifying this region position as one of the world's lowest-cost VCM producers. [9]

It is expected that VCM demand will grow at an average annual rate of 3.7% during 2015–20. Consumption of VCM will remain highly dependent upon the performance of the PVC business

As mentioned, the widespread use of PVC is the reason of the vinyl chloride great importance. Asia Pacific, particularly China, is the most significant market for PVC accounting for more than 50% of the global PVC market. Europe and North America follow as the second and third largest market for PVC. [10]

In the coming years, it is expected the PVC market to growth. High growth in the building and construction sectors, automobile industry and medical devices are the major drivers contributing the overall market growth of PVC. While increasing competition from steel and concrete pipes and

prohibited use of PVC in the construction of green building are the dominant constraints for PVC market. [10]

2.2 VCM Production Processes

The industrial production of vinyl chloride relies on two main paths [7]:

1. Hydrochlorination of acetylene;
2. Thermal cracking of 1,2-dichloroethane, also known as EDC;

The acetylene-based technology predominated until the early 1950s, when acetylene, produced via calcium carbide from coal was one of the most important basic feedstocks for the chemical industry. [11]

Ethylene became readily available at competitive prices, with the large-scale production of ethylene derived polymers and with the substantial increase of cracking capacity all over the world. [11]

Due to the energy input required to produce acetylene and the hazards of handling it, the industry has spent several decades to distance from the acetylene technology. Besides the economic disadvantage of the higher priced hydrocarbon feed, the acetylene process has the drawback of not being balanced. Also, there is a strong environmental incentive to cease the use of the mercury-based catalyst involved in the acetylene-based process. [11]

Thereafter, ethylene-based routes have since become predominant. Today, this acetylene-based process is largely obsolete outside China, where the availability of relative cheap local coal makes it still economically attractive to continue with this technology. [12].

2.2.1 VCM from EDC

Currently, the ethylene-based technology is a balanced process. This means that all intermediates and by-products are recovered in a way that ensures a tight closure of the mass balance to only VCM as the final product, starting from ethylene, chlorine and oxygen. [6]

The three main chemical steps are as follows [6] :

- Direct chlorination of ethylene to 1,2-ethylenedichloride (EDC)

$$C_2H_4 + Cl_2 \rightarrow C_2H_4Cl_2 \tag{2.1}$$

- Thermal cracking (pyrolysis) of EDC to VCM

$$C_2H_4Cl_2 \rightarrow C_2H_4Cl + HCl \tag{2.2}$$

- Recovery of HCl and oxychlorination of ethylene to EDC

$$C_2H_4 + 2HCl + \frac{1}{2}O_2 \rightarrow C_2H_4Cl_2 + H_2O \tag{2.3}$$

This way the overall balanced process may be described by the following equation:

$$C_2H_4 + 0.5Cl_2 + 0.25O_2 \rightarrow C_2H_3Cl + 0.5H_2O \tag{2.4}$$

The overall reaction is exothermal so the VCM plant should be able to cover a large part of its energy needs. [6].

Most of the chlorinated waste is produced during oxychlorination step. Therefore, employing only direct chlorination of ethylene is environmentally beneficial, but chlorine has to be recovered from the by-product HCl, as by means of the classical Deacon reaction (equation 2.5).

$$2HCl + 0.5O_2 \rightarrow Cl_2 + H_2O \tag{2.5}$$

Figure 2 shows the ethylene-based process from ethylene, chlorine and oxygen to VCM.

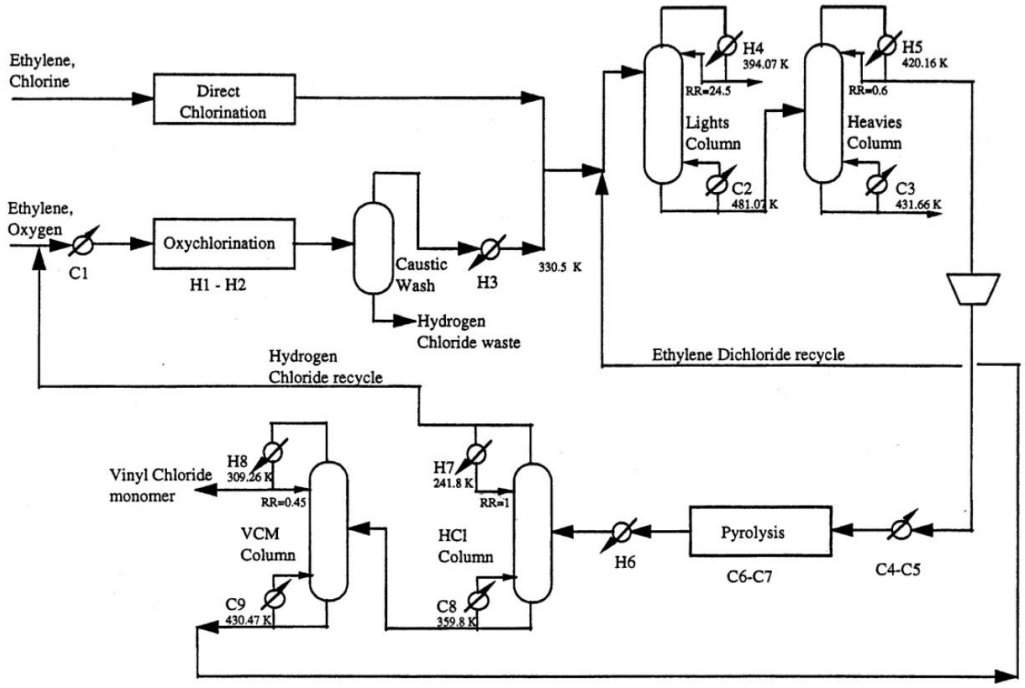

Figure 2 – EDC-based VCM production process (Adapted from [13])

Direct chlorination

The first reaction, in which occurs the direct chlorination of ethylene to EDC, is exothermic and it is desirably carried out in the liquid phase of ethylene dichloride, so there is a better control of the temperature. It occurs in the presence of a Lewis-acid type catalyst, in most cases FeCl3, in concentrations of 0.1 to 0.5 wt%. [6]

The most critical by-product in this step is the 1,1,2-trichloroethane (TCE) formed through one of the following reactions (equations 2.6 and 2.7). [6]

$$C_2H_4 + 2Cl_2 \rightarrow C_2H_3Cl_3 + HCl \tag{2.6}$$

$$C_2H_4Cl_2 + Cl_2 \rightarrow C_2H_3Cl_3 + HCl \tag{2.7}$$

Small amounts of oxygen may increase the selectivity to EDC by inhibiting the secondary reactions that originate radical, followed by the formation of Impurities. The use of high-purity reactants is essential to avoid the formation of a larger spectrum of impurities that make the EDC purification even more complicated. A slight excess of chlorine is preferred in order to ensure complete ethylene conversion. [6]

The direct chlorination step can either be conducted at low (LTC) or high temperatures (HTC). In the LTC process, ethylene and chlorine react at temperatures below the boiling point (50 to 70^{o}C). A high selectivity (over 99%) can be achieved, however rejecting the heat of reaction to the environment at low temperature is highly inefficient. Another major drawback is the catalyst removal from EDC, which is only achieved by costly operations and sources of pollution. [6]

The HTC process is carried out at the boiling point of EDC, at temperatures from 90 to 150^{o}C This way the heat of reaction, which is seven times higher than the EDC's heat of vaporization, can be used for its purification. The chemical reactor may be integrated as a re-boiler of a distillation column or designed as independent equipment. This process commonly presents a lower selectivity, however by sophisticated reactor design and the use of modified catalyst, yields comparable to the LTC can be obtained using considerably lower energy consumption. [6]

Oxychlorination

The HCl produced during the EDC cracking is recycled to the oxychlorination section, where it is used together with ethylene to produce EDC.

The highly exothermal reaction is conducted at temperatures of 200°C and pressures of 1.5 to 5 bar, in fixed-bed or fluid-bed reactors. The widely used catalyst is based on copper(II) chloride impregnated on alumina. [6]

The fluid-bed technique offers a more intense heat transfer, prevents the occurrence of hot spots and allows a more efficient catalyst regeneration. An ethylene conversion of 93–97% can be achieved with selectivity in EDC of 91–96%. However, backmixing, which influences conversion and selectivity, cannot be avoided. [11]

In the case of fixed bed reactors, the temperature is difficult to control due to the highly exothermic reaction. This problem is overcome by the dilution of the catalyst with inactive diluents. [6]

Thermal Cracking

The EDC produced in the two sections above mentioned is purified and then thermally cracked to vinyl chloride and hydrogen chloride (equation 2.2) in a pyrolysis furnace.

The pyrolysis reaction from EDC to VCM consists of complex Cl-catalysed radical and molecular reactions. Thus the molecular reaction or overall reaction described above (equation 2.2) is not representative of the actual chemical reaction steps.

The EDC cracking can be carried out in the liquid or gas phase. However, the liquid-phase process is industrially unimportant because expensive chlorine is lost as salt when EDC is treated with alkaline solution. Moreover, the aqueous process stream to be discarded presents several

environmental problems. Thus, the gas-phase route is the most industrially relevant for the production of VCM. [11]

The furnace operates at 50-60% EDC conversion, with gas residence time of about 10 to 30 seconds, pressures of 6 to 35 atm and temperatures between 480-530 ^{o}C. Higher temperatures increase the EDC conversion but cause a decrease in the selectivity. The choice of operating conditions is made based on a compromise between, for example, cost of utilities, production rate and shut down periods, among others. [3] [14]

Although it is possible to achieve a VCM selectivity of 99%, there is a fraction of by-products formed in this process which, due to large material through-put, create severe inefficiencies. The coke formation is inevitable and requires periodic shut-downs of the entire plant for its removal. Other gas-phase by-products, such as chloroprene (C_4H_5Cl) and butadiene (C_4H_6), also cause difficulties in distillation columns. One way to increase conversion while maintaining high selectivity is to allow a small amount, 1200 ppm of carbon tetrachloride (CCl_4), an oxychlorination by-product, to enter with the feed. This increases free chlorine radical formation, which increases conversion to 60%. [3] [15]

The cracked gas is then quickly quenched to avoid further decomposition of VCM, but also to remove the coke and other high-molecular impurities.

Purification Section

The effluent of the reactor goes to a purification section, where through distillation the hydrogen chloride produced is recovered to be used in the oxychlorination section. This is followed by a second distillation column to recover the VCM, where an EDC crude stream is obtained as the bottom product. The VCM obtained is submitted to further purification in order to meet the specifications

The crude EDC stream must then be purified so it can be recycled to the process. This is accomplished with two sequential distillation columns. The first one is used to separate the EDC from light impurities (e.g., butadiene, chloroprene or dichloroethylenes). In the second column, the EDC is obtained from the top, being separated from the heavy components (eg: trichloroethane).

2.3 The Cracking Furnace

Pyrolysis of EDC is an endothermic reaction (ΔH = 71 kJ/mol) that is carried out in a furnace, as previously mentioned.

The furnace is constituted by four main sections: a radiation section, a convection section, a shock section and a stack. [15]

The radiation section, also referred to as the firebox, contains the tubes, burners, and tube sheets. The heat required for the endothermic set of reactions is supplied by combustion of fuel from the firebox burners. These are in most cases fed by natural gas, though some plants use hydrogen-driven furnaces, using hydrogen from on-site chloralkali plants. [11] This section is referred as the radiation section because the temperature is so high that the main heat-transfer mechanism is radiation. [1]

In the firebox, the EDC is cracked to VCM and HCl through a first-order free radical chain mechanism, which starts with the homolytic cleavage of a C – Cl bond. The intermediate dichloroethane radical is stabilized by elimination of a chlorine radical, which propagates the chain. The radical chain is terminated by recombination (reverse reaction to initiation) or wall collisions, as it is usual for this type of reaction. [11]

As mentioned before, the temperature is kept around 500^{o}C, to minimise by-product formation. Due to the high temperatures in the cracking zone, chromium-nickel alloys are often used. [11]

After the radiation section, the resulting combustion gas flows through a shock area before passing into the convection section. Here the heat is recovered by preheating the EDC feed stream.

The combustion gases are then released to the atmosphere through the stack section.

In the convection section, EDC with purity over 99% is heated up to its boiling point and vaporised. After, the EDC feed re-enters the furnace in the shock section, where it is superheated up to cracking reaction temperature around 400 – 420 ^{o}C. In this zone, the heat transfer occurs by both radiation from the firebox and convection from the flue gas.

The structure diagram of an EDC cracker is illustrated in Figure 3.

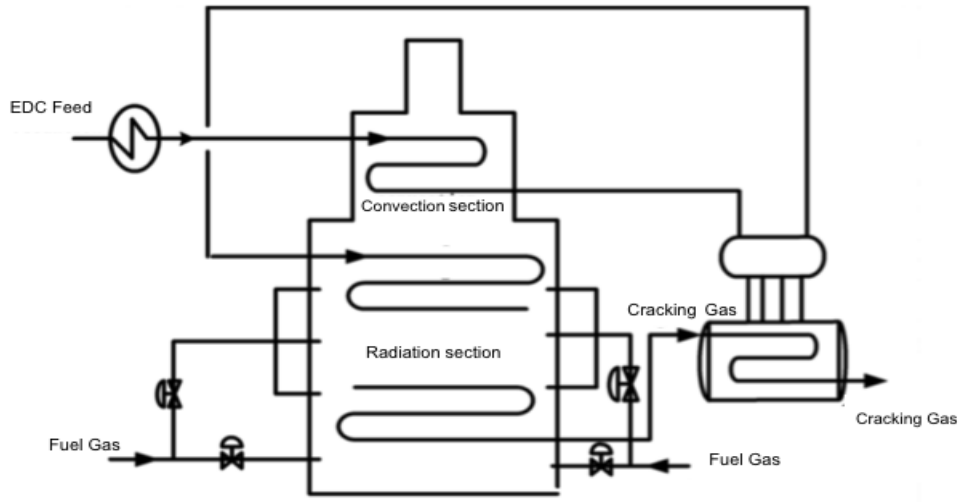

Figure 3 – EDC cracker furnace diagram [16]

2.4 Cracking kinetic mechanism

The cracking of EDC to VCM can be described by purely molecular mechanism as well as mechanisms that include radical reactions

Molecular Mechanisms

There are some molecular mechanisms that due to their simplicity assure a reduced computing time when compared to radical mechanisms. However, they fail to predict the by-products composition and, for this reason, they end up being inadequate to model the downstream separations if necessary.

Kaggerud worked on the modelling of EDC cracking, using a three dimensional CFD model representing the firebox. Only the main reactions were considered on the process side, resulting in a conversion of approximately 50% with an outlet temperature of 504 ^{o}C. [14].

Considering only the main reactions and a side reaction of VCM cracking to ethylene and hydrogen chloride, Li et al. [4] obtained results showing a slight overestimation of the conversion, with the selectivity equal to industrial data.

In Dimian and Bildea´s [6] work a purely molecular mechanism was also considered. This mechanism consisted of main reactions, the cracking of EDC to VCM, and the production of acetylene from VCM (producing HCl) and ethylene from EDC (with chlorine as a by-product).

Radical Mechanisms

The pyrolysis reactions from EDC to VCM consist of complex Cl-catalysed radical and molecular reaction. For this reason, the mechanisms involved are of great complexity and have been extensively studied. [1]

There have been several proposed mechanisms to describe the cracking reactions of EDC, which vary in terms of extent and complexity.

One of the most complex reaction mechanism was reported by Borsa (1999) [3] and consists of 71 molecular species, 64 radical species and 818 reactions. This reaction set is a comprehensive treatment of reactions consisting of species with up to four carbon atoms. This model predicts the main by-products such as acetylene, chloroprene, butadiene, ethylene and ethane. The model fails, however, to predict the formation of chloromethane and 1,1,2-trichloroethane. When comparing the results of the model with laboratory data, it can be noted that the model over-predicts EDC conversion in about 30%. [3]

In order to optimize the expenditure for the model adjustments, simplifications have been made in the view of data accuracy and less complex mechanisms have been presented.

Choi et al. (2001) [1] presented a less complex mechanism, considering 47 species, of which 22 are radicals, and 108 reactions. With this mechanism, the conversion is slightly overestimated, as well as the concentration of acetylene.

In this path for optimization, Schirmeister et al. (2009) [5] presented a model consisting of only 31 reactions, 16 stable substances and 8 radical species describing all relevant products, intermediates and by-products. This model was then used by Li et al. [16] which shows a slight over–prediction of conversion and selectivity versus plant data.

Mechanism to be implemented

In this work, the Choi mechanism is implemented to the EDC cracker model.

As previously mentioned, this mechanism consists of 108 reversible reaction and 47 species, of which 30 are molecular and 22 are radical. [1] The components list, as well as the master sets of kinetic expressions, may be found in tables 8 to 10, Appendix A.

Generally, radical reactions are divided into three main steps: initiation, propagation, and termination. However, in the case of EDC pyrolysis, these reactions are also categorized into eight main classes: [1]

1. Chain initiation reactions;
2. H abstraction reactions;
3. Cl abstraction reactions;
4. Radical addition reactions;
5. Radical decomposition reactions;
6. Purely radical reactions;
7. Purely molecular reactions;
8. Chain termination reactions;

The initiation step involves the formation of Cl radicals from molecular species. EDC is the main source of these radicals (equation 2.8), but other impurities such as CCl_4, also generate Cl radicals (equation 2.9). [1]

$$CH_2ClCH_2Cl \rightarrow CH_2ClCH_2 + Cl^{\bullet} \quad (2.8)$$

$$CCl_4 \rightarrow CCl_3 + Cl^{\bullet} \quad (2.9)$$

The H abstraction is done by the Cl radicals and represents the main propagation step. This class of reactions represents the key point for analyzing the EDC cracking reaction (equation 2.2). [1]

The Cl radical reacts with the chlorinated hydrocarbons, through the H abstraction, originating a chlorinated hydrocarbon radical. The reaction rate depends on the concentration of Cl as well as on the reaction temperature. [1]

During the radical decomposition reaction, the $CH_2ClCHCl^{\bullet}$ radical is decomposed to VCM and $Cl^{\bullet}$ radical once again (equation 2.10). [1]

$$CH_2ClCHCl^{\bullet} \rightarrow C_2H_3Cl + Cl^{\bullet} \quad (2.10)$$

Besides the radical reactions, some molecular reactions also play a significant role in the EDC pyrolysis. The molecular dehydrochlorination of EDC is a good example of this, representing a relevant path for VCM formation (equation 2.11). [1]

$$CH_2ClCH_2Cl \rightarrow C_2H_3Cl + HCl \quad (2.11)$$

A great part of the by-products is formed through a similar reaction path to the EDC pyrolysis. Acetylene is considered the main precursor of coke generation and is involved in the same mechanisms of radical and molecular reactions. This component is formed mainly via dehydrochlorination of VCM. It starts with the H abstraction from VCM by chlorinated radicals such as Cl or CH_2Cl (equations 2.12 and 2.13). [1]

$$C_2H_3Cl + Cl \rightarrow CHClCH + HCl \quad (2.12)$$

$$C_2H_3Cl + CH_2Cl \rightarrow CHClCH + CH_3Cl \quad (2.13)$$

The radical $CHClCH^{\bullet}$ formed in the first step of the mechanism is then decomposed to acetylene and Cl radical. This is the key reaction in the production of acetylene (equation 2.14). Since

the decomposition of the $CHClCH^{\bullet}$ radical is an endothermic reaction, it will be favoured by an increase of temperature. [1]

$$CHClCH^{\bullet} \rightarrow C_2H_2 + Cl^{\bullet} \tag{2.14}$$

Acetylene can also be formed through some molecular reactions from VCM (equation 2.15).

$$C_2H_3Cl \rightarrow C_2H_2 + HCl \tag{2.15}$$

The interaction of VCM or acetylene with other components represents the major path for the formation of heavy species such as butadiene, chloroprene or vinyl acetylene. [1]

2.5 Coke formation

The coke formation is inevitable during the EDC thermal cracking and its formation rate is mainly determined by two operational factors: the purity of the raw material and the heat flux distribution along the reactor. [17]

Coke deposition throughout the process from the reactor coils inside the firebox to where the gases are quenched has a significant impact on the process efficiency.

First, considering that the coke layer is a poor heat conductor, coke formation leads to decreased furnace thermal efficiency, requiring a higher temperature in the firebox to maintain EDC conversion at the desired level. [3]

Furthermore, increased coke thickness will increase skin temperature of the reactor, which is the main limitation of coil metallurgy. [3]

Moreover, the increase in coke layer thickness reduces the cross-section of the reactor tube. With a constant EDC feed rate, the pressure drop along the tubes increases and the residence time decreases. When the pressure drop gets to a certain level, the process is stopped and the coke is removed, in a process known as decoking. [3]

Finally, coke particles entrained in the gas need to be removed from the liquid stream after the quenching to avoid plugging and other problems in downstream units.

Reduced EDC cracking conversion and increased maintenance and utility costs are other results of the coke formation phenomenon. These problems force plant operators to shut down the unit for decoking process, which normally takes up to three days. [1]

Hence, predicting the run length of the furnace is essential, both to maximise it, avoiding unnecessary strain to the coil, and to enable a reliable planning schedule, preventing expensive storage of intermediate products. Typically, a run length of a commercial EDC cracker is 1 to 2 years, which depends on the type of reactor, feedstock, and operating conditions [16] or until the coil wall temperatures rise over 650^{o}C [5].

According to Borsa et al. [3], catalytic coke formed from reactive hydrocarbons on metal surfaces does not occur. Instead, coke formation begins with the formation of tar droplets. Tar droplets form from coke precursors at high temperature in the pyrolysis furnace and are transported through the heat exchanger to the quench tower. Tar droplets impinge on the tube wall surfaces where they

undergo dehydrogenation, originating coke. It is also stated that chloroprene is the only chemical species strongly correlated with total coke formation. Thus it is considered the main coke precursor.

These conclusions follow the ones made by Mochida et al. [18], who identified two types of coke. The first is an anisotropic pyrolytic carbon produced in the cracker reactor. For this kind of coke, acetylene and butadiene are referred as the main precursors of coke.

The second type of coke is isotropic granules agglomerated into dense carbon bodies in the transfer line exchangers before and after the reactor. In this case, the coke may be formed from reactive species with boiling points around 300°C.

Li et al. [17] presented a coking mechanism that considers acetylene as the only coke precursor, using the radical scheme from Schirmeister et al. [5] (equation 2.16)

$$C_2H_2 + 2Cl^{\bullet} \rightarrow 2C + 2HCl \tag{2.16}$$

As mentioned before, the coke formation during the EDC cracking is inevitable. However, some studies were done in order to reduce its formation.

Following this line, there are a few patents suggesting coating the coil walls to reduce coke deposition.

According to Jo et al. [19] coke formation is inhibited by coating the surfaces with a boron compound, while Tong [20] recommends the use a phosphine compound. Dreher et al. [11] also claims that coking formation is inhibited by adding 1,1,2-trichloroethane.

Decoking

As already discussed, the procedure adopted to remove the coke deposited is called decoking.

Since removing coke by mechanical techniques is not feasible, the usual process consists in burning the coke out with a mixture of steam and air [21].

First, the furnace is taken off-line and the residual hydrocarbons are purged downstream with steam, while the process flow goes to a particular decoking system. Steam–air mixture is then introduced into the radiant coils to burn out the coke at temperatures of about 800°C. To avoid the overheating of the radiant coil, it is important to carefully increase the air concentration. In modern furnaces, the CO_2 content is measured continuously during decoking and the air flowrate is adjusted accordingly. The decoking of the radiant coils is complete after approximately 20h. [21]

Once the radiant coil is clean, the removal of the coke deposited in the TLE is carried out, which takes about 36h. [21]

In modern plants, the off-gases leaving the radiant coil during decoking are directly sent to the TLE which is then decoked as a result. However, it is always necessary, at least once a year, to perform a mechanical cleaning of the heat exchanger(s). [21]

An increase of the furnace length means higher productivity and, consequently, higher profits. Because of this, the optimization of the operating conditions of the furnace plays a key role in increasing the overall process profitability.

3. Materials and Methods

This work was performed in gPROMS ProcessBuilder developed by Process Systems Enterprise Ltd. In this chapter the main features of this software are described.

3.1 gPROMS ProcessBuilder® software

In this work, the models were created and simulated in gPROMS ProcessBuilder software, developed by Process Systems Enterprise.

The gPROMS® advanced process modelling platform is a powerful equation-oriented modelling and optimization tool on which all of PSE's gPROMS® products are built. [22]

The gPROMS® platform provides drag & drop flowsheeting, custom modelling, parameter estimation, physical properties integration and powerful optimization tools that allow direct calculation of optimal solutions rather than by trial-and-error simulation. [22]

Besides the integral parts of gPROMS®, it is also possible to use external software components, which provide a range of computational services to the models. These are defined as parameters named Foreign Object (FO) and include physical properties packages, external unit operation modules, or even complete computational fluid dynamics (CFD) software packages. [22]

3.2 Multiflash

Multiflash is the standard gPROMS® physical properties package, supplied by KBC Advanced Technologies.

Multiflash is a highly rigorous properties package, which supports all commonly-used thermodynamic and transport properties, including a wide range of equations of state and activity coefficient thermodynamic models. [23]

It is specially designed for equation-orientated modelling, granting tight convergence of internal iterations and analytical partial derivatives regarding the temperature, pressure and composition. This is achieved with a Multiflash input file (.mfl), in which all the components, physical properties models, among other things that are necessary to the problem, are defined. This file is created using a graphical interface of Multiflash for Windows to be imported into Process Builder afterwards. [23]

3.3 Large Scale Kinetic Mechanisms (LSKM)

A stoichiometric matrix has a total of elements of $[\mathrm{No.\ of\ Components}] \times [\mathrm{No.\ of\ Reactions}]$. If the kinetic mechanism by Choi et al. is considered the stoichiometric matrix would have 5076 elements

(47 components × 108 reactions). A problem of this size would require a rather extensive computing time.

However, since these matrixes are sparse (most of the elements are zero), they can be compressed to only the significant values, i.e. the non-zero elements.

The LSKM Foreign Object is a package designed to allow an efficient representation of large-scale reaction mechanisms in gPROMS. It is used to compress a kinetic mechanism by eliminating the non-zero elements, according to the scheme reported by Tewarson [24]

One packed form of storing a sparse matrix is to store only the non-zero elements, alongside with necessary indexing information. There are four advantages of using this kind of packed form: [24]

- Larger matrices can be stored and handled in the internal storage of the computer, in other case impossible.
- It is quicker to obtain the data from the compressed form, which is an advantage when using external storage devices.
- Only the non-trivial operations are performed, which saves a substantial amount of computation time.
- The usage of this packed form can be particularly advantageous in multiplying several row and column vectors, useful in linear programming, for example.

Sparse matrix Treatment

For the LSKM FO, the second compression scheme reported by Tewarson [24] was implemented. In this scheme the matrix is stored in three arrays:

- VE (Value of Elements) – contains all the non-zero values of the matrix.
- RI (Row Indexes) – Has the same number of elements as VE and stores the row indexes where the value from VE used to be located.
- CIP (Column Index Pointer) – If the first non-zero element of the α^{th} column is in position n_α in the RI array, then that value is stored in the α^{th} element of CIP, i.e. CIP(α) = n

Having this in mind, the matrix M will be stored as follows.

$$M = \begin{bmatrix} 0 & 0 & 0 & n_{14} & 0 & 0 \\ n_{21} & 0 & n_{23} & 0 & 0 & n_{26} \\ 0 & 0 & 0 & 0 & 0 & 0 \\ 0 & n_{42} & 0 & n_{44} & 0 & 0 \\ 0 & 0 & 0 & 0 & n_{55} & n_{56} \end{bmatrix}$$

$$VE = [n_{21} \quad n_{42} \quad n_{23} \quad n_{14} \quad n_{44} \quad n_{55} \quad n_{26} \quad n_{56}] \tag{3.1}$$

$$RI = [2 \quad 4 \quad 2 \quad 1 \quad 4 \quad 5 \quad 2 \quad 5] \tag{3.2}$$

$$CIP = [1 \quad 2 \quad 3 \quad 4 \quad 6 \quad 7] \tag{3.3}$$

Whether it is intended to extract n_{44}, the first step should be to look at CIP, where $CIP(4) = 4$ and $CIP(5) = 6$. This means both $VE(4)$ and $VE(5)$ contain values from the forth column. Since $RI(5) = 4$, it is possible to conclude that the value of the element in the forth column and forth row corresponds to $VE(5)$.

3.4 ReadData Foreign Object

With the ReadData FO, it is possible to add more information besides the one given by the LSKM FO. This information is obtained from a .txt file, from which is converted into arrays. In this .txt file, the line containing a string will become the array's name and the following lines will become the data.

This tool allows the user to introduce in the model information regarding the components, such as molecular weight, enthalpy and entropy of formation, as well as necessary parameters to calculate the fluid's heat capacity.

These files are not only used alongside with the LSKM scheme, but they can also be useful in other applications that require information to be provided this way.

3.5 State Estimation

State estimation is a widespread and well-established technique in control engineering and weather forecasting. However, its usage combined with advanced process models is not so common, especially in the chemical and petrochemical industry.

There is a wide variety of different applications, ranging from process control to on-line model adjustment, which require on-line estimates and predictions of an evolving set of variables, given uncertain data and dynamics.

If on-line data of some output variables are available, a state estimator can adjust the model prediction using these measurements to obtain a better estimate of the state. This is the most important application of on-line state estimation according to Simon. [25]

In gPROMS the Extended Kalman Filter algorithm is adopted, since it is considered to be one of the simplest and most important tools for state estimation purposes. [25]

During state estimation, the model receives on-line measured data regarding the input and output variables. For each time unit, the estimator updates the output variable according to a prediction/correction approach. Firstly, there is the prediction step, where model equations are taken into account, followed by the correction step, where available measurements are used to correct the predicted state estimate. Hence for each instant the model will give two values for the output, resulting from each of these steps.

For each measured output variable and model parameter a variance is defined. The variance set to the parameters can be interpreted as a measure of how much its initial value can change during

state estimation, in order to meet the objective. A higher variance will allow larger change to the parameter value in comparison to a smaller variance.

On the other hand, the variance of the plant data can be seen as a measure of the confidence the model can have on it. A smaller variance indicates more accuracy of the measurement and state estimation would give more importance to such measurements in comparison to those with higher variance.

To implement this technique in gPROMS, two files are required. The first is a configuration file, where all the parameters, inputs and output variables to be considered are specified, as well as their variances. The second file is a text file that contains all the plant data regarding the input and output variables.

4. Model Set-up

The objective of this work was to set-up the EDC cracker model (EDCM2) using the already existing furnace model libraries[1] within gPROMS ProcessBuilder.

For this to be possible, some changes had to be done in these libraries, as well as the creation of new sub-models. Such changes and developments are presented in this Chapter.

4.1 Furnace Model

The EDC cracker was set-up using the furnace model libraries within gPROMS Process Builder, represented in Figure 4.

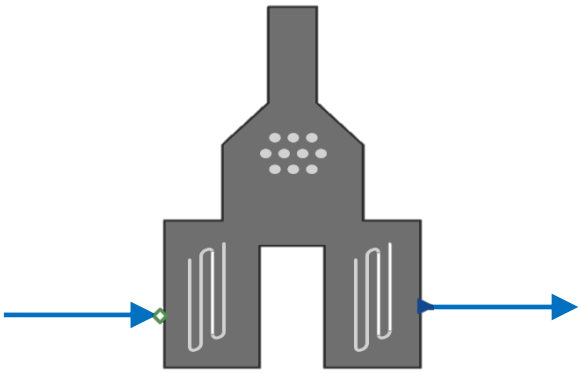

Figure 4 – Furnace icon in gPROMS Process Builder

The furnace model comprises of several sub models, consisting of three mains sections:

- Convection Section – Where the EDC stream is heated;
- Radiant Section (Coil) – Where cracking reactions occur;
- Transfer Line Exchanger (TLE) – Where the coil outlet stream is quickly quenched to prevent degradation of the highly reactive product through secondary reactions;

The radiant section consists of multiple coils operating in parallel. In the furnace model, each coil is assumed to behave the same and one representative coil is modelled.

Figure 5 shows the structure of the furnce model. Following are main submodels:

- Convection Section (Vapour Preheater)
- Radiant Coil
- TLE

[1] Library – The models are categorized into sections that are presented to the user as model libraries

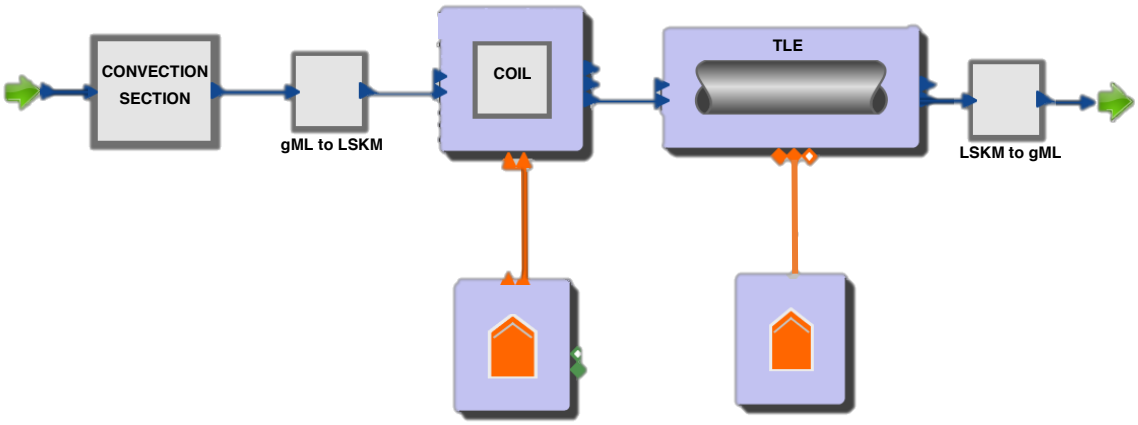

Figure 5 – Furnace Mode within gPROMS ProcessBuilder

Both the convection section and the coil models consist basically of several cracking tube models.

In the convection section, whose model configuration is presented in Figure 6, precedes the coil model and includes three cracking tubes. The first two are used to heat up the gas, while the third one corresponds to an adiabatic section.

The Coil model is presented in Figure 7 and consists mainly of six cracking tubes. In this coil model, the first and the last tubes correspond to adiabatic sections outside the radiant box. The remain 4 tube section models are used to represent the full length of the actual reactor.

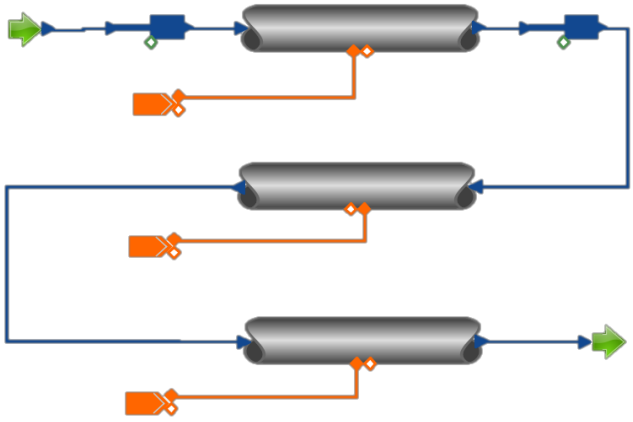

Figure 6 – Convection Section (Vapour preheater model)

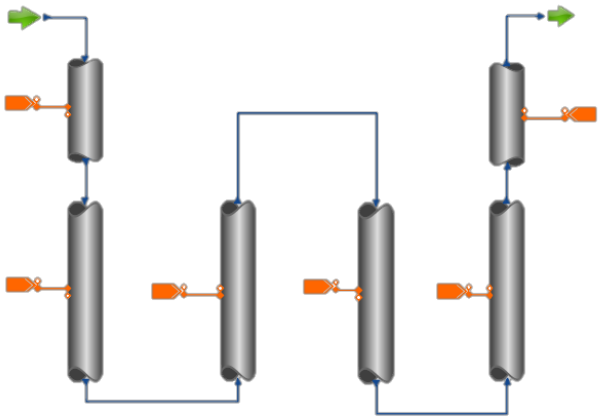

Figure 7 – W-coil model

In the furnace dialogue box[2] all the inputs to the model can be specified. These inputs include:

- Geometry and configuration of the elements that constitute the furnace;
- Operating conditions (inlet or outlet pressure, temperature, flowrate and composition);

[2] Dialogue box – Window that pops up on the screen when the user clicks on the model icon, with options that the user can select or fields to fill in.

- Cracking and Coking kinetics;

The cracking kinetics for EDC cracking as reported by Choi et al. (2001) [1] was implemented and integrated to the furnace model.

All the kinetic parameters were given to the model through a LSKM scheme.

4.2 Cracking Tube

In the cracking tube model, it is assumed a one-dimensional plug flow due to the turbulent flow, as well as low viscosity for the reaction side stream.

The sub models of the cracking tube include:

- Cracking kinetic model
- Coking kinetic model
- Fluid properties model
- Heat transfer coefficient model
- Friction factor coefficient model

4.2.1 Cracking kinetic Model

The cracking model is used to determine the reaction rate. According to the Choi mechanism [1], all the reactions that occur are reversible. Thus the global reaction rate (r_j) is given by the difference between the forward (f) and reverse (r) rates (equation 4.1).

$$r_j = k_{fj} \prod_{k=1}^{NC} {C_i}^{n_{f,kj}} - k_{rj} \prod_{k=1}^{NC} {C_k}^{n_{r,kj}} \quad (4.1)^3$$

In these equations k_{fi} and k_{ri} are the kinetic constants for the forward and reverse reactions respectively, $n_{f,ij}$ and $n_{r,ij}$ are the reaction orders and C_i is the concentration of component i.

The kinetic constants for the forward reactions ($k_{f,j}$) are calculated according to the equation 4.2.

$$k_{f,j} = A_j T^{b_j} \exp\left(\frac{-E_{a,j}}{R.T}\right) \quad (4.2)$$

Where T is the fluid's temperature (K), A_j is the pre-exponential factor, $E_{a,j}$ is the activation energy of reaction j and b_j is the temperature exponent used to correct deviations from the Arrhenius equation.

The kinetic constant for the reverse reaction is determined using the equilibrium constant (equation 4.3). The equilibrium constant is calculated from the change of standard entropy (ΔS_j^0) and enthalpy (ΔH_j^0) during the reaction at system's temperature (T) and pressure (P), according to equation 4.4.

[3] NC – Number of components

$$K_{cj} = \frac{k_{fj}}{k_{rj}} \tag{4.3}$$

$$K_{cj} = exp\left(\frac{\Delta S_j^0}{R} - \frac{\Delta H_j^0}{RT}\right)\left(\frac{P}{RT}\right)^{\sum_{i=1}^{NC} n_{r,ij} - n_{f,ij}} \tag{4.4}$$

4.2.2 Coking kinetic Model

The coking model was also developed during the present work.

For this model, it was considered that coke is formed through the dehydrogenation of Tar. Tar droplets form at high temperature in the pyrolysis furnace and are transported through the heat exchanger to the quench tower. When these droplets impinge on the wall surface, they suffer dehydrogenation, originating coke [5]. Thus the coking reaction rate is considered to be the reaction rate of tar dehydrogenation.

In the coking model, the mass balance for Tar is done according to equation 4.5. The concentration of Tar is given by the difference between the Tar that is formed and is consumed by dehydrogenation.

$$\frac{\partial}{\partial z}(G.w_{Tar}.A) = \left[r'''_{tar\ formation}(z)\ A(z)\right] - \left[r''_{tar\ dehydrogenation}(z)\ 2\pi\ r_i(z)\right] \tag{4.5}$$[4]

The reaction rate of Tar formation (equation 4.6) is a function of acetylene and chloride concentrations since it was concluded that the influence of other coking promoters was negligible as described in Chapter 2.

$$r_{tar\ formation}(z) = k_{tar\ formation} C_{C_2H_2}(z) C_{Cl}(z) \tag{4.6}$$

$$r_{tar\ dehydrogenation}(z) = k_{tar\ dehydrogenation} C_{TAR}(z) \tag{4.7}$$

Both kinetic constants for Tar formation (equation 4.8) and Tar dehydrogenation (equation 4.10) follow the Arrhenius equation. The values for the activation energies and pre-exponential factors were obtained from a previous project done by PSE (EDCM1), where the kinetic constants were tuned to the data.

$$k_{tar\ formation}(z) = k^{T_{ref}}{}_{tar\ formation}\ e^{\frac{-E_{tar\ formation}}{R}\left(\frac{1}{T(z)} - \frac{1}{T_{ref}}\right)} \tag{4.8}$$

$$k_{tar\ dehydrogenation}(z) = k^{T_{ref}}{}_{tar\ dehydrogenation}\ e^{\frac{-E_{tar\ dehydrogenation}}{R}\left(\frac{1}{T(z)} - \frac{1}{T_{ref}}\right)} \tag{4.9}$$

4.2.3 Fluid Properties Model

The fluid properties Model is used to determine all the properties required for the cracking tube model.

Multiflash does not support radical species and their properties. For this reason, two sub-models are called whether it is using a molecular-based mechanism or a radical one.

[4] A – Cross sectional area (m^2)
G – Mass flux ($kg/m^2\ s$)

When using the molecular properties model, the Multiflash FO is used to get the information regarding the following properties of the mixture:

- Density;
- Viscosity;
- Thermal Conductivity;
- Heat Capacity;
- Enthalpy;
- Components molecular weight;

In the case of a radical-based mechanism, the required properties are imported using the ReadData foreign object. From this file, the model receives the following properties for each component:

- Molecular weight (M_w);
- Enthalpy of formation (ΔH_f);
- Entropy of formation (ΔS_f);
- Parameters for heat capacity calculation (a_0, a_1, a_2 and b);

The enthalpy of the mixture is calculated based on the components enthalpy of formation, according to equation 4.10.

$$\Delta H = \sum_{i=1}^{NC} \left[\Delta H_{f,i} \times w_i\right] + \overline{C_p}\left[T(z) - T_{ref}\right] \tag{4.10}$$

Where T_{ref} is the reference temperature (298.15 K) and $\overline{C_p}$ is the average heat capacity of the mixture, given by the weighted average of the heat capacities of each component (equation 4.11).

$$\overline{C_p} = \sum_{i=1}^{NC} \frac{C_{p,i} \times w_i}{M_{w,i}} \tag{4.11}$$

The heat capacity of each component is determined using a 3rd order polynomial fitting as shown in equation 4.12.

$$\begin{aligned} C_{p,i} &= \int_{T_{ref}}^{T} a_0.T^3 + a_1.T^2 + a_2.T + b.dT \\ &= \frac{\left[\frac{a_0}{4}\left(T(z)^4 - {T_{ref}}^4\right) + \frac{a_1}{3}\left(T(z)^3 - {T_{ref}}^3\right) + \frac{a_2}{2}\left(T(z)^2 - {T_{ref}}^2\right) + b(T(z) - T_{ref})\right]}{T(z) - T_{ref}} \end{aligned} \tag{4.12}$$

Due to the lack of data, and considering the small concentration of radicals and by-products, the remaining properties (viscosity and thermal conductivity) were obtained using Multiflash for the main components (EDC, VCM and HCl).

4.3 Temperature Profile Model

Accurate representation of temperature profile along the coil is important to get accurate yield predictions.

In previous works, the temperature in the process was determined by the heat balance based on the flowrates of the flue gas, fuel and air fed to the furnace. [26]. In that case, it would be possible to obtain the same inlet and outlet temperatures as in the real unit. However it would be difficult for the model to predict exactly the same temperature profile, which strongly affects the results.

In this work, a model was developed where the temperature profile is determined by polynomial approximation, according to equation 4.13. This is achieved by considering as inputs to the model five real temperature measurements (T1 to T5 in Figure 8) as well as the respective axial positions. Besides this, the model also receives the Coil Inlet Temperature (CIT) from the upstream process simulation that corresponds to axial position zero.

$$T(z) = a + b.z + c.z^2 + d.z^3 + e.z^4 + f.z^5 + g.z^6 \tag{4.13}$$

Considering only the last two temperature measurements (T4 and T5 in Figure 8), a linear extrapolation is applied in order to predict the temperature for axial position equal to 1 (T6 in Figure 8). By having the sixth temperature, the model is able to calculate the remaining constants of the equation 4.13 and determine the temperature profile inside the coil. Figure 8 shows the temperature profile in the coil, where the CIT appears in green, the five temperature measurements in blue and in purple is the sixth temperature determined by the linear extrapolation.

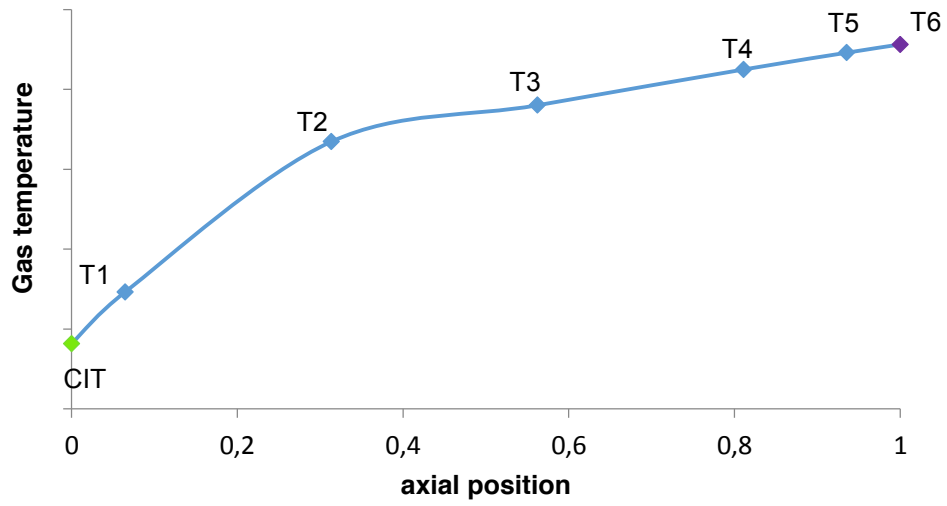

Figure 8 – Temperature Profile in the coil representation

In this model, it is assumed this temperature profile is maintained by controlling the fuel feeding rate at the furnace side.

Temperature increases very rapidly up to 30% of the total length. The EDC pyrolysis reaction is known to start at about 700 K, which is achieved around that point. Since then the rate of increase is lower because heat is predominantly used for the endothermic reaction and not for the elevation of temperature from that position. The temperature reaches approximately 760-780 K at the outlet of reactor.

5. Simulation Results

Following the EDC cracker model set-up, it was necessary to test the performance and accuracy of the model (EDCM2). In this chapter the simulation results are presented and validated.

5.1 Model Size

EDCM2 has a considerable size, as it can be seen in Table 1 that shows the number of variables that constitute the model.

Table 1 – Number of variables in the model EDCM2 (Model Size)

Type of Variable	Number
User-defined	371053
After identity Elimination	209065
After model pruning	170317
Differential	165

5.2 Simulation (start of run conditions)

In a previous work, an EDC cracker model (EDCM1) was developed by PSE to simulate a specific industrial system. Since it was considered that the model accurately described the system, at an early stage, EDCM1 was used to validate the results from the EDC cracker model developed in the present work (EDCM2).

To make this comparison possible, the required input variables were exactly the same in both models. These input variables are the following:

- Feed composition and flow rate;
- Coil inlet pressure (CIP);
- Process gas temperatures – Temperature Profile Interpolation Model;

It was considered that the furnace feed was mainly EDC (>99 wt%) and a small amount of CCl_4. Carbon tetrachloride is known to be an efficient source of Cl radical and it can be used to promote the pyrolysis reaction. However, the Cl radical also acts as a promoter for undesirable coke formation so its concentration should be limited. [1].

Regarding the output, this analysis was done focusing on the variables considered relevant to describe the good behaviour of the model, which are the following:

- Conversion of EDC;
- Outlet composition;
- Pressure Drop;

The results for EDC conversion and outlet composition will reflect the accuracy of the cracking kinetic model. Regarding the outlet composition, besides acetylene, only the two main components were considered (EDC and VCM) since they alone 80% of the total. Acetylene was only considered in this analysis due to its relevance for the coking model.

The pressure drop is mainly affected by coking deposition, thus it can be used as an indication of the efficiency of the coking kinetic model implemented in this work.

Along with the input variables already pointed out, the cracking and coking kinetics are also inputs given to the model. As mentioned before, in the present work (EDCM2) the cracking kinetics from Choi et al. [1] were implemented. However, in the EDCM1 the cracking kinetics used were the same but tuned according to the real data from the plant.

On the other hand, the coking kinetics were strictly the same in both models. The values for the activation energies and pre-exponential factors were obtained from the previous project done by PSE (EDCM1), where the kinetic constants were tuned to the data.

In Table 2, the deviations between the results of the two models are presented.

Table 2 – Relative and absolute errors between the predictions from the EDCM2 developed in the present work and EDCM1 (Choi kinetics tuned to the real data)

Output Variable		**Units**	**EDCM1**	**EDCM2**	**Absolute error**	**Relative error (%)**
EDC conversion		%	58.2	58.9	0.7	1.2
Outlet Composition	EDC	%wt	41.7	40.9	-0.8	-1.9
	VCM		36.5	37.0	0.5	1.4
	C_2H_2		0.048	0.025	-0.023	-47.9

If in EDCM1, the kinetics used were purely the ones from Choi [1] all these deviations would be within 0.2%. Thus the deviations from EDCM1 with tuned kinetics and EDCM2 result from the difference between the cracking kinetics.

EDCM2 under-predicts the acetylene composition in about 50% when compared to the EDCM1 results with the tuned kinetics, as shown in Table 2. As acetylene is relevant for the coking formation, this discrepancy will have an impact on the pressure drop predictions.

It was then verified that the reaction rate for Tar formation from acetylene in EDCM2 was in average 3.5 times lower than the one predicted by EDCM1 (equation 5.1).

$$r_{Tar\ formation\ from\ acetylene}(\mathrm{EDCMl}) = 3.5 \times r_{Tar\ formation\ from\ acetylene}(\mathrm{EDCM2}) \quad (5.1)$$

Having this in consideration, the value of 3.5 was used as a factor to be multiplied by the kinetic constant of Tar formation from acetylene. The influence of this scaling factor is presented in the next subchapter.

5.3 Simulation of a cycle (Dynamic Simulation)

After evaluating the start of run simulation results, simulation of a complete cycle is performed, considering a period of around 12 months. The model inputs for the simulation were obtained from plant data and the cracking kinetics from Choi et al. were used.

This case differs from the first analysis since the inputs are not fixed as before but change over the time according to the data from the real unit.

The input variables analysed are the same as the ones mentioned before. While for the output variables, in this validation the outlet flowrates of the main components were considered instead of the outlet composition.

Considering the significant discrepancy in the acetylene concentration previously presented, for the coking kinetics two cases were considered (case A and B), which are presented in table 3.

Case A considers the coking kinetics previously described and already used for EDCM1 and EDCM2. In case B, the scaling factor influence is tested, so the coking kinetics are the same as in case A but having the kinetic constant for tar formation from acetylene multiplied by 3.5.

Table 3 – Description of the two cases considered for simulating the complete cycle

	Case A	**Case B**
Cracking kinetics	Choi et al. (2001)	Choi et al. (2001)
Coking kinetics	Parameters used in EDCM1	Same as Case A, but: $k_{Tar\ from\ acetylene} = 3.5 \times k_{Tar\ from\ acetylene}(\mathrm{EDCM1})$

The model predictions for cases A and B were then compared to the available plant measurements, as it can be seen in Figures 9 to 12. For the first 20% of the cycle, data corresponding to the output variables was not considered as reliable.

Figure 9 shows the pressure drop predictions for both cases as well as the data from the real plant.

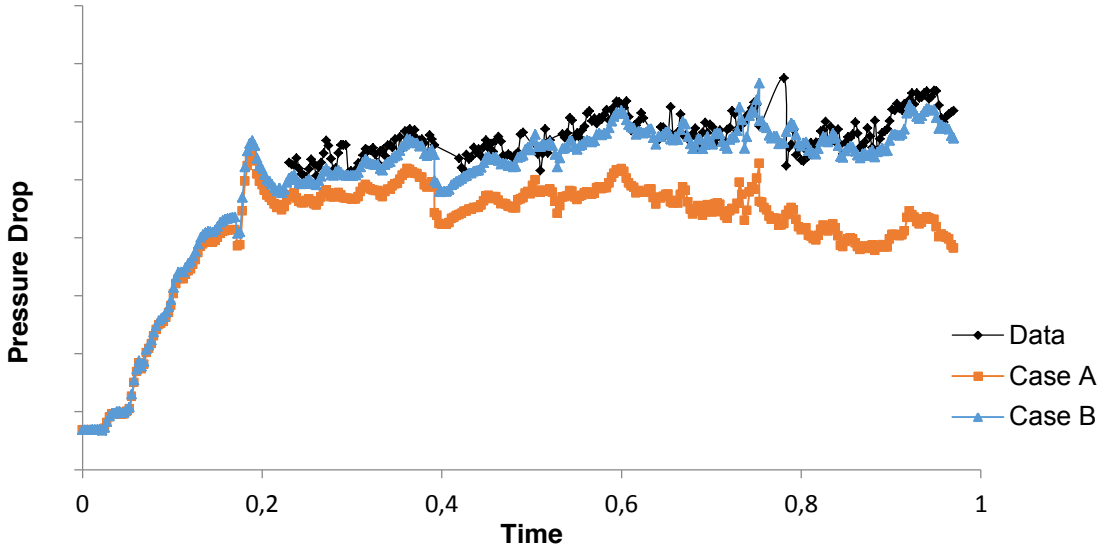

Figure 9 – Coil pressure drop predictions for case A and case B against real Data with time being normalised.

In case B due to the scaling factor considered, the coke formation is higher than in case A and the pressure drop in the coil increases with time. For this reason, the results from case B are better matched to the data, presenting an average deviation of 1.8% against 9.1% from case A.

The effect of scaling factor on outlet flow rate predictions are not significant (<0.1%) as presented in the figures below (Figure 10 to 13). In fact, it is verified for all the components that the results from case B present a slightly higher average deviation than case A The average deviation between model predictions and real data is shown in Table 4.

Figure 10 shows the model predictions for EDC outlet flowrate from case A and B and the respective real data.

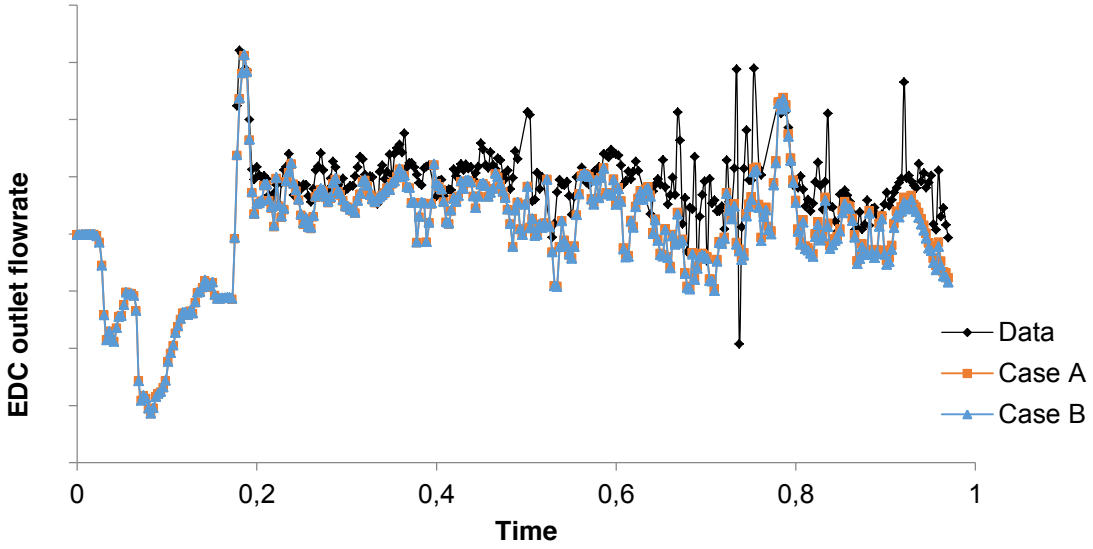

Figure 10 – EDC outlet flowrate predictions for case A and case B against real Data with time being normalised.

The predictions have an average deviation of 4.4% and 4.5%, for case A and B, respectively. From this figure, it is verified that the flow rate predicted by the model is in general lower than the real data suggesting over prediction of EDC conversion.

EDC conversion was calculated according to the equation 5.2, for both cases A and B, as well as for the real data. The EDC inlet was obtained from the real unit data which was used as an input to the model. The EDC outlet corresponds to the model predictions in each case.

$$\text{Conversion}_{\text{EDC}} = \frac{\text{EDC}_{\text{inlet}} - \text{EDC}_{\text{outlet}}}{\text{EDC}_{\text{inlet}}} \tag{5.2}$$

Figure 11 shows EDC conversion over time determined based on the results from cases A and B. For both cases, the EDC conversion is higher than the one calculated from the data in about 3.3%.

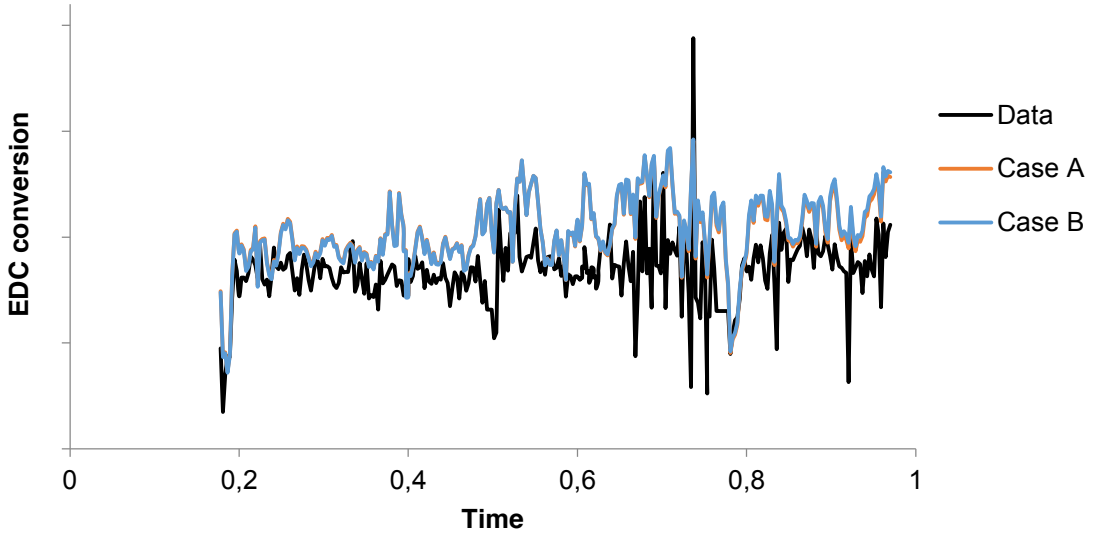

Figure 11 – EDC conversion in the outlet of the coil over time for case A and B and real data with time being normalised.

In figure 12 the results for VCM outlet flowrate are presented. The model predictions have an average deviation from the real data of 1.8% for both cases. The model predicts in average a higher VCM outlet flow rate as it would be expected since the model over predicts the EDC conversion.

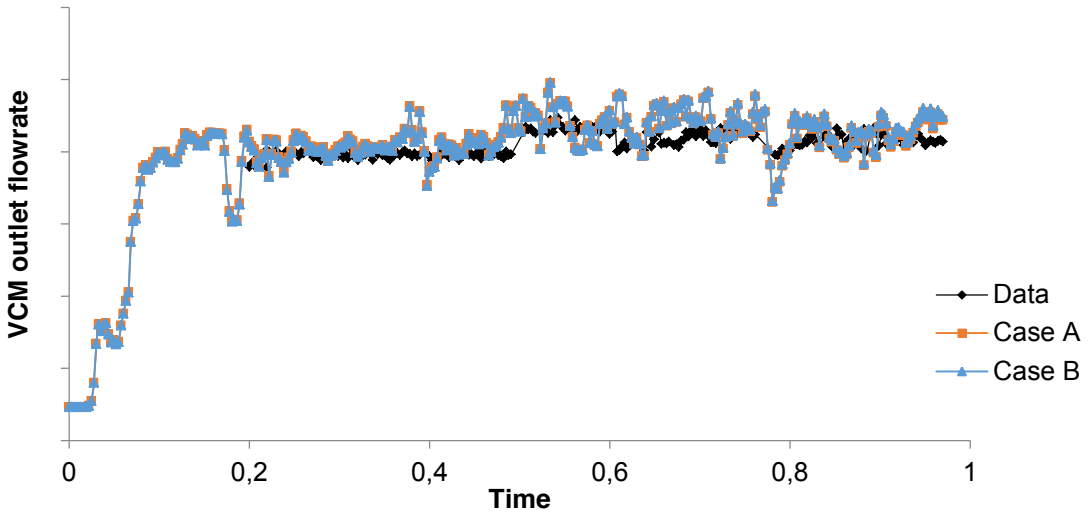

Figure 12 – VCM outlet flowrate predictions for case A and case B against real Data with time being normalised.

Table 4 presents the average deviation from the model predictions and the real data for each output variable for both cases.

Table 4 – Average deviation from real data for each output variable predictions in case A and B.

	Case A (%)	**Case B (%)**
Pressure drop	9.1	1.8
EDC outlet flowrate	4.4	4.5
VCM outlet flowrate	1.8	1.8

A sensitivity analysis was also performed considering higher and lower values for the corrective factor, though it was concluded that 3.5 was actually the one presenting the best fit to the data.

6. State Estimation

Following the comparison of model prediction with real data, state estimations were attempted in order to test the feasibility of improving the model predictions.

In state estimation, the objective is to adjust the model predictions to the real data, by changing some chosen related parameters.

To apply this technique, it is necessary to set variances for each adjusted parameter and the data corresponding to the output variables.

The variance in the case of the parameters can be seen as a measure of how much the model can vary its initial value, in order to meet the objective. A higher variance will allow larger change to the parameter value in comparison to a smaller variance.

On the other hand, the variance of the real data is associated to the measurements uncertainty. It can be seen as a measure of the confidence the model can have on it. A smaller variance indicates more accuracy of the measurement and state estimation would give more importance to such measurements in comparison to those with higher variance.

Table 5, shows the variances of parameter and output variable measurement used in the state estimation runs. The plant data used for state estimation is pressure drop and the parameter to be adjusted is "coking reaction rate adjustment" (CRR_{adj}).

The adjusted parameter is being multiplied to the expression used to calculate the coking reaction rate, as indicated by its name (equation 6.1)

$$r_{coke\ formation} = r_{tar\ dehydrogenation} \times CRR_{adj} \tag{6.1}$$

Table 5 – Variances of parameter and measurements used in state estimation runs

Type	Parameter/Variable Name	Variance	
		SE[5] Case 1	SE[5] Case 2
Adjusted Parameter	Coking reaction rate adjustment	5×10^{-6}	5×10^{-7}
Output variable measurement	Pressure drop	5×10^{-6}	5×10^{-6}

For CRR_{adj}, an initial value of 1 is set, so if state estimation is not being employed, this value does not change, hence it will not affect any result. During state estimation, the value of this parameter is changed so as to obtain better estimates pressure drop. If this parameter increases, the coke formation will increase, leading to an increase in pressure drop. The decrease of this parameter will have the opposite effect.

[5] SE – State Estimation

Two cases were considered to be presented in this analysis (SE case 1 and 2), that vary from one another only in the variance defined to the coking reaction rate adjustment.

Following the line of thought described above, in case 1 the model is allowed to make more significant changes in the coking reaction rate adjustment parameter.

The following charts (figure 13 to 16) show the model predictions with state estimation for both cases, regarding pressure drop, coke reaction rate adjustment and EDC and VCM outlet flowrates, The model predictions without state estimation (Simulation) are also presented, so it is possible to verify if state estimation has improved, or not, the results when compared to the real data.

Similarly to chapter 5, the data corresponding to the first 20% of the cycle was considered to be unreliable. In addition to that, for state estimation purposes, only the first 70% of the cycle was considered.

Figure 13 shows the state estimation results for pressure drop. The model predictions are similar for cases 1 and 2, with average deviations from real data of about 2.6% and 2.8%, respectively, as shown in table 6. Both cases show improvements when compared with the results without state estimation, which presents an average deviation of 4.1% (table 6).

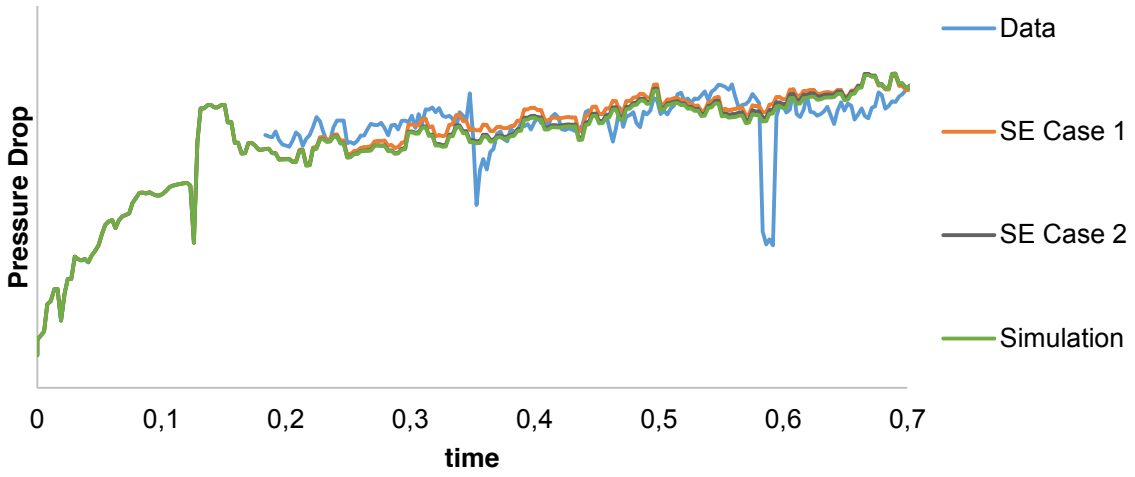

Figure 13 – Pressure drop predictions from state estimation against real data with time being normalised

Despite the proximity of the results from case 1 and 2, the first one is still able to present better predictions. This is in agreement with what was expected since in case 1 the model has more freedom to change the coking rate parameter in order to adjust the pressure drop predictions to the data.

Figure 14 shows the evolution of the reaction rate adjustment parameter over time. In the Simulation case there is no change of this parameter from its initial value since the model is not doing any state estimation.

For the other two cases, it can be seen that the parameter does not vary at the beginning of the cycle. This is because in that period there is no data for pressure drop. Considering the model is only working towards the pressure drop adjustment if there isn't any data the model does not change the parameter.

As it was expected, in case 1 the coking reaction rate adjustment parameter will have more significant oscillations, since the set variance is higher than in case 2.

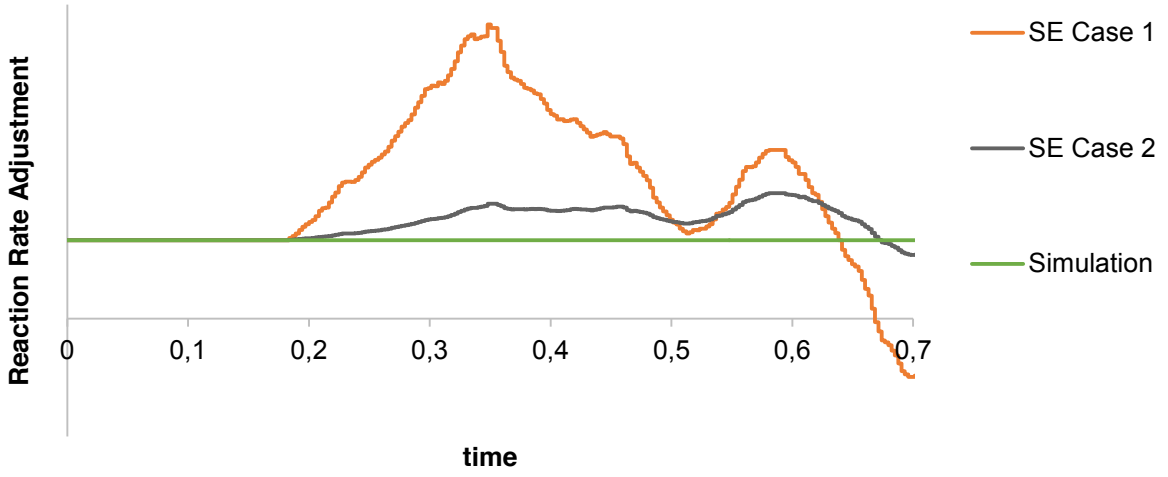

Figure 14 – Coking reaction rate adjustment parameter variation from state estimation

As the pressure drop increases, the model intensifies the coke formation, by increasing the coking reaction rate adjustment parameter.

At some point, around 35% of the period, the data shows a lower peak in pressure drop. Thus the model responds similarly by decreasing the parameter.

Around 50% of the time, the parameter starts to increase again until another decrease in pressure drop occurs (around 58% of the time). The parameter continues decreasing since then, even assuming negative values at the end of the cycle.

The fact the parameter has a negative value means the coking reaction rate is also negative, which in reality would represent coke dissipation. Obviously in a real system, after being formed, coke will not disappear unless the operation is stopped and a decoking process is implemented.

In case 2, it can be verified the parameter has a similar behaviour than in case 1, but with oscillations of lower amplitude. Contrary to case 1, the parameter never reaches negative values.

Therefore, it is possible to verify that the variance settings on measurements and parameters are important to get meaningful values of the adjusted parameters such as in case 2.

For all the two components the results with state estimation (cases 1 and 2) show improvements when compared to the Simulation case.

In figure 15, the results for EDC outlet flow rate are presented. Case 1 and 2 have average deviations of 5.3% and 5.5%, respectively. Without state estimation, the model predictions present an average deviation of 6.3%.

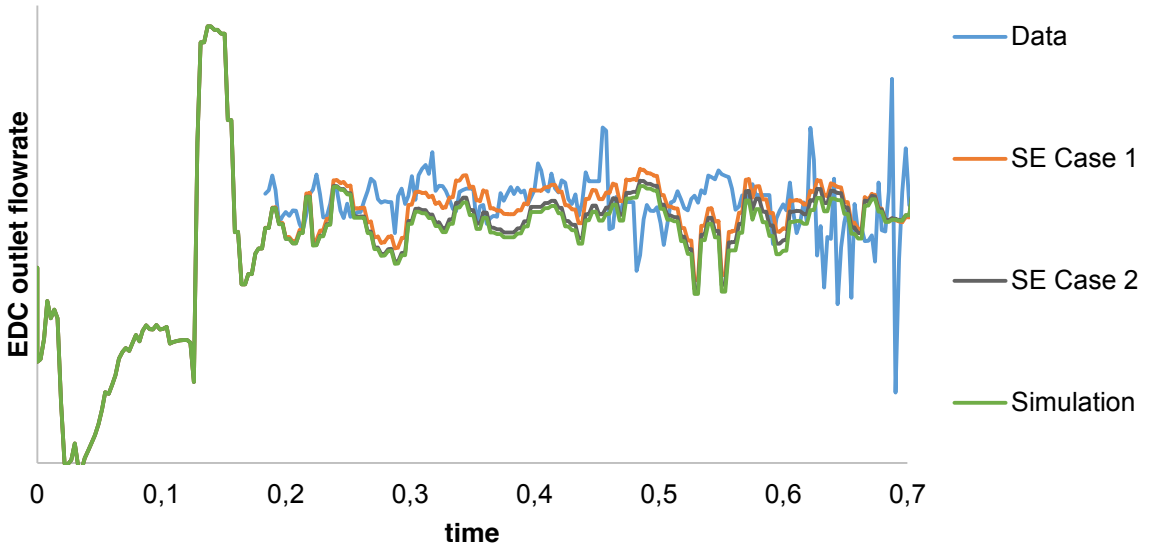

Figure 15 – EDC outlet flowrate predictions from state estimation against real data

Figure 16 shows the results for VCM outlet flow rate. For this component, the model predictions present an average deviation of 3.4% for case 1 and 3.1% for case 2. The predictions without state estimation have an average deviation of 4.2%, which is, as expected, higher than the other two cases.

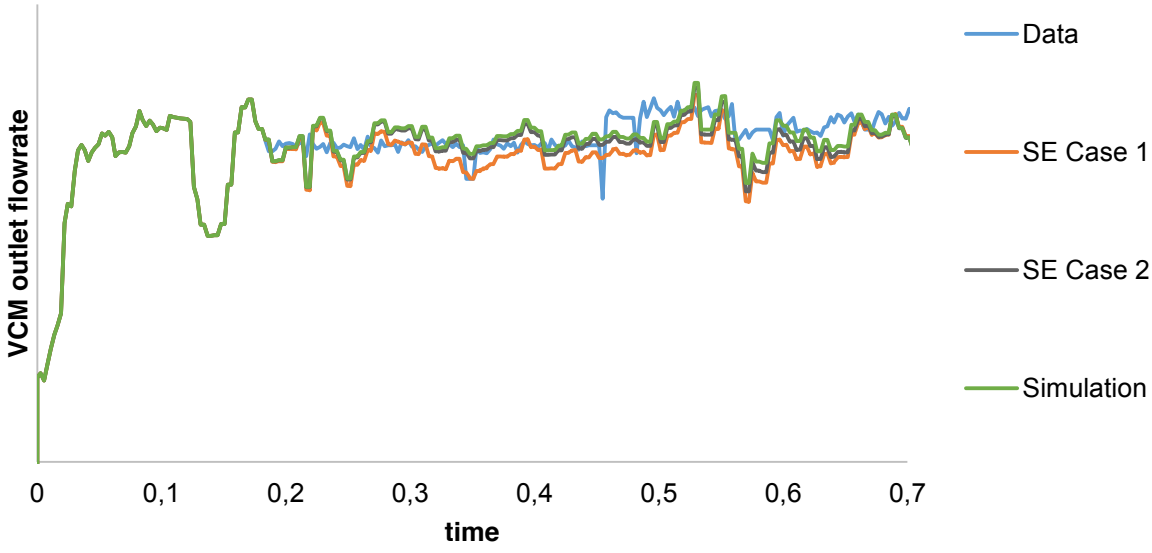

Figure 16 - VCM outlet flowrate predictions from state estimation against real data with time being normalised

Table 6 shows the average deviations of the model predictions from real data, for each case considered and output variable. It is also presented the improvement on the results by varying the adjusted parameter.

Table 6 – Average deviations (%) of state estimation predictions from the real data for each case and variable, as well as the improvement relatively to the simulation case.

	Case 1		**Case 2**		**Simulation**
	Average deviation (%)	Improvement (%)	Average deviation (%)	Improvement (%)	Average deviation (%)
Pressure Drop	2.58	43.3	2.76	39.2	4.54
EDC outlet flowrate	5.28	16.1	5.54	12.0	6.29
VCM outlet flowrate	3.38	5.09	3.12	12.3	3.56

7. Kinetic Reduction

As a final step in this work, a study regarding the possibility of reducing the cracking kinetic scheme was attempted. The objective was to verify if all the 108 reactions included in the mechanism are in fact essential for the proper modelling of the furnace.

In this study, effect of each reaction (except the main reactions) on key output variables are analysed by disabling those reactions from the scheme.

The key output variables considered in this study are:

- EDC conversion and selectivity
- Outlet composition (considering the whole set of components)

Allowing a deviation of 0.1% from the model results when considering all the reactions, it would be possible to exclude 48 reactions. These reactions are presented in table 7 with the respective reaction class.

Table 7 – Reactions that may be excluded by class of reactions

Reaction Class	Class name	Reactions to be excluded	reactions to be excluded / total of reactions
1	Chain initiation	3, 4, 6, 8, 9 & 11	6 / 11
2	H abstraction	14, 16, 19,22, 24, 25, 26, 27, 30, 32, 34, 36, 37, 38, 39, 42, 43 & 47	18 / 38
3	Cl abstraction	52, 57, 59, 60 & 68	5 / 21
4	Radical addition	72	1 / 5
5	Radical decomposition	---	0 / 5
6	Purely radical	81 & 82	2 / 2
7	Purely molecular	83 & 85	2 / 5
8	Chain termination	90, 91, 92, 93, 94, 95, 96, 97, 98, 99, 102, 104, 106 & 107	14 / 21

It is important to point out that the reactions previously present are the ones that when excluded didn't affect the results more than 0.1% for any of the 54 variables considered. This was verified, even when all 48 reactions were excluded simultaneously

In the furnace feed stream, there were only ethylene dichloride and carbon tetrachloride present. Hence it is not possible to conclude if these reactions would not be relevant in case there were more impurities in feed.

It would be necessary to test that possibility, by including in the feed other components that may be present as impurities.

8. Discussion and Conclusions

In this work, an EDC cracker model (EDCM2) was setup using the furnace model libraries within gPROMS ProcessBuilder, to model the VCM production through EDC cracking.

In a previous work, an EDC cracker model (EDCM1) was developed by PSE to model a specific industrial unit. Since it was considered that EDCM1 is able to accurately simulate the reality of that unit, in an early stage, was used to validate the results from EDCM2. The same inputs were given to both models, excepting for the cracking kinetics. This difference lead to deviations between the results from the two models (table 2).

It was verified that EDCM2 under predicts acetylene outlet composition in about 50% when compared to EDCM1. Considering the relevance of this component as the main coke precursor, such deviation will have an impact on the pressure drop prediction, predominately affected by coke deposition. It was then verified that the coking reaction rate in EDCM2 was 3.5 times lower than EDCM1. Thus the value of 3.5 was used as a factor to be multiplied to the kinetic constant of Tar formation from acetylene.

Following this analysis, the model predictions from (EDCM2) was compared against data from a real plant such as pressure drop and the outlet flow rate of the main components (EDC and VCM).

Two cases were considered (cases A and B), similar to each other in all the aspects, except for the coking kinetics. In case B the reaction rate of coking formation is 3.5 times higher than in case A, by considering the scaling factor above mentioned. A sensitivity analysis was also performed considering higher and lower values for this scaling-factor, though it was concluded that 3.5 was actually the one presenting the best fit to the data.

The increment of coke formation in case B leads to an increase in pressure drop prediction with time. Thus the results from case B, with an average deviation of 1.8%, fit better the data than case A where pressure drop does not increase as much, presenting a deviation of 9.1%.

When analysing the model predictions for the outlet flowrate of the main components, it can be verified that these are not significantly affected by the factor applied in case B. The average deviations between both cases predictions and the real data are similar for all the components.

State estimations were also performed, focusing on the adjustment of pressure drop predictions by changing the coking reaction rate adjustment parameter. The model predictions were then compared to the results without state estimation (Simulation).

For all the output variables analysed, the results with state estimation (cases 1 and 2) show improvements when compared to the Simulation case. Cases 1 and 2 differ from one another in the variance defined for the adjusted parameter.

Pressure drop presents average deviations of 2.6 and 2.8% with state estimation, while the normal simulation would give results with about 4% of deviation.

EDC outlet flow rate presents average deviations of 5.3% and 5.5% for case 1 and 2, respectively. Without state estimations, the deviation would be 6.3%.

For VCM outlet flow rate the deviations are less significant than the previous component. In the Simulation case the results have an average deviation of about 4%, which is improved by state estimation reaching deviations of less than 3.5%.

Overall, with state estimation, it is possible to improve the model predictions for all the output variables. The variable for which state estimation had a more significant impact is, as expected, pressure drop with an improvement of around 40%. For the outlet flowrates improvements between 5 and 20% were achieved (table 6).

Even though the Case 1 is the one presenting an higher improvement in the accuracy of pressure drop predictions, that is achieved by taking the reaction rate adjustment parameter to not realistic values. Therefore, it is concluded that the variance settings on measurements and parameters are important to get meaningful values of the adjusted parameters.

The final step of this work was to study the possibility of reducing the cracking kinetic scheme. Allowing a deviation of 0.1% from the results considering the original mechanism, it was verified that 48 reactions could be excluded without compromising the results.

In the feed stream, only ethylene dichloride and carbon tetrachloride were considered for simulation purposes. However, the furnace feed may contain other components formed as by-products in the upstream process, predominately during oxychlorination. Some key impurities formed during that step are 1,1,2-trichloroethane, trichloroethylene, 1,1 and 1,2-dichloroethylenes, ethyl chloride, chloromethanes (methyl chloride, methylene chloride, chloroform), as well as polychlorinated high-boiling components [6]. Hence it was not possible to conclude if these reactions would not be relevant in case there were more impurities in feed.

8.1 Future Work

Despite the work done, several improvements may and should be made to the model developed. This would include further testing of state estimation for the full cycle using fine tuning the different variances for the measurements and adjusted parameters. Further fine tuning of the state estimator could be performed by using data from multiple cycles.

It is also necessary to continue the kinetic reduction study initialized. In order to conclude about its feasibility, more tests would have to be done, considering other possible impurities in the furnace feed, such as chloroform, methyl chloride, ethyl chloride and 1,1,2-trichloroethane.

State estimation with the reduced kinetic scheme is expected to improve the computational performance significantly.

9. References

[1] B.-S. Choi, J. S. Oh, S.-W. Lee, H. Kim and J. Yi, “Simulation of the Effects of CCl4 on the Ethylene Dichloride Pyrolysis Process,” *Industrial & Engineering Chemistry Research,* 2001.

[2] “ChemicalSafetyFacts.org,” [Online]. Available: https://www.chemicalsafetyfacts.org/polyvinyl-chloride-post/. [Accessed October 2017].

[3] A. G. Borsa, “Industrial Plant/Laboratory Investigation and Computer modeling of 1,2-Dichloroethane pyrolysis,” 1999.

[4] C. Li, G. Hu, W. Zhong, H. Cheng, W. Du and F. Qian, “Comprehensive Simulation and Optimization of an Ethylene Dichloride Cracker Based on the Onde-Dimensional Lobo_Evans Method and Computational Fluid Dynamics,” *Industrial & Engineering Chemistry Research,* 2013.

[5] R. Schirmeister, J. Kahsnitz and M. Trager, “Influence od EDC severity on the Marginal Costs of Binyl Chloride Production,” Industrial & Engineering Chemistry Research, 2009.

[6] A. C. D. a. C. S. Bildea, “Vinyl Chloride Monomer Process,” in *Chemical Process Design: Computer-Aided Case Studies*, Weinheim, WILEY-VCH Verlag GmbH & Co. KGaA, 2008, pp. 200-228.

[7] H. A. Manfred Rossberg, H. A. Wilhelm Lendle and H. A. Gerhard Pfleiderer, Chlorinated Hydrocarbons, Weinheim: Wiley-VCH Verlag GmbH & Co. KGaA, 2006.

[8] “Analysis in Vinyl Chloride (VCM) Production Process,” APPLIED ANALYTICS.

[9] I. Markit, “Vinyl Chloride Monomer,” IHS Markit, November 2015. [Online]. Available: https://www.ihs.com/products/vinyl-chloride-monomer-chemical-economics-handbook.html. [Accessed March 2017].

[10] “PVC Market: Global Industry Analysis and Forecast to 2020,” Persistence Market Research, 2017. [Online]. Available: http://www.persistencemarketresearch.com/market-research/pvc-market.asp . [Accessed March 2017].

[11] E. Dreher, T. R. Torkelson and K. K. Beutel, “Chloroethanes and Chloroethylenes,” in *Ullmann's Encyclopedia Of Industrial Chemistry*, Wiley–VCH, 2012.

[12] CHEMSYSTEMS, “Vinyl Chloride Monomer (VCM) / Ethylene Dichloride (EDC),” Nexant Inc., 2009.

[13] A. Lakshmanan, W. Rooney and L. Biegler, “A case study for reactor network synthesis: the vinyl chloride process,” *Computers & Chemical Engineering,* 1998.

[14] T. H. Kaggerud, “Modeling an EDC Cracker using Computational Fluid Dynamics (CFD),” 2007.

[15] J. Dry, B. Lawson, P. Le, I. Osisanya, D. Patel and A. Shelton, “Vinyl Chloride Production,” university of Oklahoma, 2003.

[16] C. Li, G. Hu, W. Zhong, W. He and W. Du, “Coke Deposition Influence Based on a Run Length Simulation of a 1,2-Dichloroethane Cracker,” *Industrial & Engineering Chemistry Research,* pp. 17501-17516, 2013.

[17] C. Li, G. Hu, W. Zhong, H. Cheng, W. Du and F. Qian, “Comprehensive Simulation and Optimization of an Ethylene Dichloride Cracker Based on the Onde-Dimensional Lobo_Evans Method and Computational Fluid Dynamics,” *Industrial & Engineering Chemistry Research,* 2012.

[18] I. Mochida, T. Tsunawaki, C. Sotowa, Y. Korai and K. Higuchi, “Coke Produced in the Commercial Pyrolysis of Ethylene Dichloride into Vinyl Chloride,” *Industrial & Engineering Chemistry Research,* 1996.

[19] D. Jo, J. Bae, J. Kim, S. W. KIM, B. Oh and S. HA Back, “Method of inhibiting coke formation in ethylene dichloride pyrolysis cracker”. Patent US7132577 B2, 2006.

[20] Y. Tong, “Phosphine coke inhibitors for EDC-VCM furnaces”. Patent US6454995 B1, 2002.

[21] H. Zimmermann and R. Walzi, “Ethylene,” in *Ullmann's Encyclopedia of Industrial Chemistry*, 2012.

[22] “The gPROMS platform,” Process Systems Enterprise, [Online]. Available: https://www.psenterprise.com/products/gproms/platform. [Accessed 20 05 2017].

[23] “Physical Properties,” Process Systems Enterprise, [Online]. Available: https://www.psenterprise.com/products/gproms/physprops. [Accessed 20 5 2017].

[24] R. P. Tewarson, “Sparse Matrices,” in *Mathematics in Science and Engineering*, Academic, 1973.

[25] D. Simon, Optimal State Estimation, Wiley, 2006.

[26] R. Wong, “Advanced modeling of vinyl chloride monomer production via thermal cracking of ethylene dichloride,” 2014.

[27] “Chemical Economics Handbook,” November 2015. [Online]. Available: https://www.ihs.com/products/vinyl-chloride-monomer-chemical-economics-handbook.html.

[28] G. Bano, “State estimation techniques for on-line model adaptation: A case study in thermal cracking,” 2015.

Appendix A – Cracking Mechanism

Components List

For the Choi mechanism implementation, the species presented in tables 8 and 9 were considered.

Table 8 – Molecular components list

Name	Chemical Formula
Methane	CH_4
Acetylene	C_2H_2
Ethylene	C_2H_4
Ethane	C_2H_6
Hydrogen chloride	HCl
Methyl chloride	CH_3Cl
Vinyl acetylene	C_4H_4
Butadiene	C_4H_6
Chloroethyne	C_2HCl
Vinyl chloride	C_2H_3Cl
Ethyl chloride	C_2H_5Cl
Chlorine	Cl_2
Dichloromethane	CH_2Cl_2
1-chlorobutadiene	C_4H_5ClS
Chloroprene	C_4H_5ClU
Dichloroacetylene	C_2Cl_2
Cis-1,2-dichloroethene	CHClCHCl
1,1-dichloroethene	CCl_2CH_2
Ethylene dichloride	CH_2ClCH_2Cl
1,1-dichloroethane	CH_3CHCl_2
Chloroform	$CHCl_3$
Dichlorobutadiene	$C_4H_4Cl_2$
1,2-dichlorobut-3-ene	$C_4H_6Cl_2$
Trichloroethylene	C_2HCl_3
1,1,2-trichloroethane	$CH_2ClCHCl_2$
Carbon tetrachloride	CCl_4
Tar	---

Table 9 – Radical components list

Chemical Formula
H
CH_3
C_2H_3
C_2H_5
Cl
CH_2Cl
C_4H_5U
C_4H_5S
CHClCH
CH_2CCl
CH_2ClCH_2
CH_3CHCl
$CHCl_2$
C_4H_6Cl
CHClCCl
$CH_2ClCHCl$
CCl_3
$C_4H_5Cl_2U$
$C_4H_5Cl_2S$
$CHCl_2CHCl$

Table 10 - Reactions that take part in the cracking mechanism with the respective kinetic constants (A – frequency factors [1/s] for unimolecular reactions and [cm^3/mol.s] for bimolecular reactions; b – exponent of temperature; E – activation energy [cal/mol]) [1]

no.	reaction	*A*	*b*	*E*
	Class 1. Chain Initiation Reactions			
1	$CH_2ClCH_2Cl=CH_2ClCH_2 + Cl$	1.01×10^{28}	−4.6	86509.0
2	$C_2H_3Cl=C_2H_3 + Cl$	1.71×10^{38}	−7.1	96370.0
3	$CH_2Cl_2=CH_2Cl + Cl$	1.02×10^{16}	0.0	76800.0
4	$CHCl_3=CHCl_2 + Cl$	0.60×10^{16}	0.0	71000.0
5	$CCl_4=CCl_3 + Cl$	1.00×10^{16}	0.0	70000.0
6	$CH_3Cl=CH_3 + Cl$	1.26×10^{37}	−6.9	90540.0
7	$C_4H_6Cl_2 + M=C_4H_6Cl + Cl + M$	1.00×10^{16}	0.0	66600.0
8	$C_4H_5ClS + M=C_4H_5S + Cl + M$	1.00×10^{16}	0.0	85900.0
9	$C_4H_5ClU + M=C_4H_5U + Cl + M$	1.00×10^{16}	0.0	94900.0
10	$C_2H_5Cl=C_2H_5 + Cl$	1.00×10^{16}	0.0	86200.0
11	$CH_2ClCHCl_2=CH_2ClCHCl + Cl$	1.00×10^{13}	0.0	77000.0
	Class 2. H Abstraction Reactions			
12	$CH_2ClCH_2Cl + Cl=CH_2ClCHCl + HCl$	1.00×10^{13}	0.0	3100.0
13	$CH_2ClCH_2Cl + CH_2Cl=CH_2ClCHCl + CH_3Cl$	1.16×10^{11}	0.0	9000.0
14	$CH_4 + CH_2ClCHCl=CH_2ClCH_2Cl + CH_3$	1.00×10^{5}	2.0	25933.0
15	$C_2H_3Cl + CH_2Cl=CH_2CCl + CH_3Cl$	1.79×10^{1}	3.6	9620.0
16	$C_2H_3Cl + CH_2Cl=CHClCH + CH_3Cl$	1.79×10^{1}	3.6	14480.0
17	$C_2H_3Cl + Cl=CH_2CCl + HCl$	1.20×10^{14}	0.0	13300.0
18	$C_2H_3Cl + Cl=CHClCH + HCl$	1.20×10^{14}	0.0	13300.0
19	$CH_2ClCH_2 + CH_3Cl=C_2H_5Cl + CH_2Cl$	1.00×10^{6}	2.0	11408.0
20	$C_2H_5Cl + Cl=CH_2ClCH_2 + HCl$	2.50×10^{7}	2.0	680.0
21	$CH_3Cl + Cl=CH_2Cl + HCl$	9.30×10^{6}	2.4	3300.0
22	$CH_3Cl + CH_3=CH_2Cl + CH_4$	1.26×10^{11}	0.0	11600.0
23	$CH_4 + Cl=CH_3 + HCl$	2.08×10^{8}	1.8	2650.0
24	$CH_3Cl + CHCl_2CHCl=CH_2ClCHCl_2 + CH_2Cl$	1.00×10^{6}	2.0	14158.0
25	$C_2H_4 + CH_2Cl=C_2H_3 + CH_3Cl$	2.00×10^{12}	0.0	12000.0
26	$C_2H_3Cl + CH_3=CH_2CCl + CH_4$	1.08×10	3.9	10490.0
27	$C_2H_3Cl + CH_3=CHClCH + CH_4$	1.08×10	3.9	12490.0
28	$C_2H_3Cl + CHCl_2=CH_2Cl_2 + CHClCH$	1.00×10^{6}	2.0	20158.0
29	$C_2H_3Cl + CHCl_2=CH_2Cl_2 + CH_2CCl$	1.00×10^{6}	2.0	17608.0
30	$C_4H_4Cl + HCl=C_4H_5ClS + Cl$	1.00×10^{6}	2.0	18283.0
31	$C_4H_5Cl_2U + HCl=C_4H_6Cl_2 + Cl$	1.00×10^{6}	2.0	29833.0
32	$C_4H_5U + CH_3Cl=C_4H_6 + CH_2Cl$	1.00×10^{5}	2.0	21733.0
33	$C_4H_5U + HCl=C_4H_6 + Cl$	1.00×10^{6}	2.0	23233.0
34	$C_4H_5S + HCl=C_4H_6 + Cl$	1.00×10^{6}	2.0	35158.0
35	$C_2H_4 + Cl=C_2H_3 + HCl$	1.00×10^{14}	0.0	7000.0
36	$C_2H_5Cl + CH_3=CH_2ClCH_2 + CH_4$	4.40×10^{2}	3.2	10340.0
37	$C_2H_5Cl + CH_3=CH_3CHCl + CH_4$	4.40×10^{2}	3.2	9340.0
38	$C_2H_3Cl + CHCl_2CHCl=CHClCH + CH_2ClCHCl_2$	1.00×10^{6}	2.0	22408.0
39	$C_2H_3Cl + CHCl_2CHCl=CH_2CCl + CH_2ClCHCl_2$	1.00×10^{6}	2.0	19858.0
40	$C_2H_3Cl + CHClCCl=CHClCH + CHClCHCl$	1.00×10^{6}	2.0	13708.0
41	$C_2H_3Cl + CHClCCl=CH_2CCl + CHClCHCl$	1.00×10^{6}	2.0	11358.0
42	$C_2H_3Cl + CH_2ClCH_2=CHClCH + C_2H_5Cl$	1.00×10^{6}	2.0	19558.0
43	$C_2H_3Cl + CH_2ClCH_2=CH_2CCl + C_2H_5Cl$	1.00×10^{6}	2.0	17008.0
44	$C_2H_3Cl + CH_3CHCl=CHClCH + C_2H_5Cl$	1.00×10^{6}	2.0	24616.0
45	$C_2H_3Cl + CH_3CHCl=CH_2CCl + C_2H_5Cl$	1.00×10^{6}	2.0	20608.0
46	$CH_2ClCHCl + C_2H_4=CH_2ClCH_2Cl + C_2H_3$	1.00×10^{6}	2.0	19258.0
47	$C_2H_6 + CH_2ClCHCl=CH_2ClCH_2Cl + C_2H_5$	1.00×10^{6}	2.0	13408.0
48	$CH_2ClCHCl + C_2H_3Cl=CH_2ClCH_2Cl + CHClCH$	1.00×10^{5}	2.0	22408.0
49	$CH_2ClCHCl + C_2H_3Cl=CH_2ClCH_2Cl + CH_2CCl$	1.00×10^{6}	2.0	19858.0
	Class 3. Cl Abstraction Reactions			
50	$CH_2ClCH_2Cl + Cl=CH_2ClCH_2 + Cl_2$	1.00×10^{7}	2.0	28108.0
51	$CH_2ClCH_2Cl + CH_2Cl=CH_2ClCH_2 + CH_2Cl_2$	1.00×10^{6}	2.0	11283.0
52	$CH_2ClCH_2Cl + CH_3=CH_2ClCH_2 + CH_3Cl$	4.00×10^{5}	2.0	16908.0
53	$CCl_4 + CH_3=CCl_3 + CH_3Cl$	1.26×10^{12}	0.0	9900.0
54	$CCl_4 + Cl=CCl_3 + Cl_2$	1.00×10^{14}	0.0	20000.0
55	$C_2H_3Cl + CCl_3=C_2H_3 + CCl_4$	1.00×10^{6}	2.0	27808.0
56	$C_4H_6Cl_2 + Cl=C_4H_6Cl + Cl_2$	1.00×10^{7}	2.0	17908.0
57	$C_4H_5ClS + Cl=C_4H_5S + Cl_2$	1.00×10^{7}	2.0	27900.0
58	$C_4H_5ClU + Cl=C_4H_5U + Cl_2$	1.00×10^{7}	2.0	36900.0
59	$C_4H_5U + HCl=C_4H_5ClU + H$	1.00×10^{6}	2.0	28858.0
60	$C_4H_5S + HCl=C_4H_5ClS + H$	1.00×106	2.0	41533.0
61	$CH_3 + C_2H_3Cl=CH_3Cl + C_2H_3$	3.00×10^{11}	0.0	17983.0
62	$C_2H_3Cl + CHClCCl=C_2H_3 + C_2HCl_3$	1.00×10^{6}	2.0	14233.0
63	$C_2H_3Cl + CH_2CCl=C_2H_3 + CCl_2CH_2$	1.00×10^{6}	2.0	13783.0
64	$C_2H_3Cl + CH_2ClCH_2=C_2H_3 + CH_2ClCH_2Cl$	1.00×10^{6}	2.0	17758.0
65	$C_2H_3Cl + CH_3CHCl=C_2H_3 + CH_3CHCl_2$	1.00×10^{6}	2.0	21508.0
66	$Cl_2 + C_2H_3=C_2H_3Cl + Cl$	5.24×10^{12}	0.0	−480.0
67	$CH_2ClCHCl + CH_3Cl=CH_2ClCHCl_2 + CH_3$	1.00×10^{11}	0.0	17950.0
68	$CH_3CHCl_2 + CH_2ClCHCl=CH_3CHCl + CH_2ClCHCl_2$	1.00×10^{6}	2.0	16783.0
69	$CH_2ClCHCl + C_2H_3Cl=CH_2ClCHCl_2 + C_2H_3$	1.00×10^{12}	0.0	18550.0
70	$CH_2ClCHCl + Cl_2=CH_2ClCHCl_2 + Cl$	1.00×10^{12}	0.0	6175.0

Table 10 (cont.) – Reactions that take part in the cracking mechanism with the respective kinetic constants (A – frequency factors [1/s] for unimolecular reactions and [cm3/mol.s] for bimolecular reactions; b – exponent of temperature; E – activation energy [cal/mol]) [1]

no.	reaction	*A*	*b*	*E*
	Class 4. Radical Addition Reactions			
71	$C_2H_2 + C_2H_3 \rightarrow C_4H_5U$	7.94×10^{8}	0.0	6900.0
72	$C_2H_2 + C_2H_3 \rightarrow C_4H_5S$	7.94×10^{8}	0.0	6900.0
73	$C_2H_3Cl + C_2H_3 \rightarrow C_4H_6Cl$	2.28×10^{27}	- 4.6	11778.0
74	$C_2H_3Cl + C_2H_3 \rightarrow C_4H_6 + Cl$	2.13×10^{8}	1.7	9157.0
75	$C_2H_3Cl + CH_2CCl \rightarrow C_4H_5ClS + Cl$	7.94×10^{13}	0.0	12844.0
	Class 5. Radical Decomposition Reactions			
76	$CH_2ClCHCl \rightarrow C_2H_3Cl + Cl$	1.58×10^{13}	0.0	20600.0
77	$CHClCCl \rightarrow C_2HCl + Cl$	3.82×10^{28}	- 5.0	37441.0
78	$CHClCH \rightarrow C_2H_2 + Cl$	1.50×10^{13}	0.0	23000.0
79	$C_4H_5Cl_2U \rightarrow C_4H_5ClU + Cl$	3.00×10^{13}	0.0	37000.0
80	$C_4H_6Cl \rightarrow C_4H_6 + Cl$	3.00×10^{13}	0.0	41600.0
	Class 6. Pure Radical Reactions			
81	$CH_2CCl + C_2H_3 \rightarrow C_4H_5S + Cl$	3.46×10^{11}	0.0	10443.0
82	$C_2H_3 + CH_2ClCHCl \rightarrow C_4H_6Cl + Cl$	1.41×10^{14}	0.0	10416.0
	Class 7. Pure Molecular Reactions			
83	$CH_2ClCH_2Cl \rightarrow C_2H_3Cl + HCl$	1.43×10^{12}	- 0.7	58920.0
84	$C_2H_3Cl \rightarrow C_2H_2 + HCl$	2.75×10^{17}	- 1.3	69312.0
85	$C_4H_6Cl_2 \rightarrow HCl + C_4H_5ClS$	3.98×10^{10}	0.0	49000.0
86	$C_4H_6Cl_2 \rightarrow HCl + C_4H_5ClU$	3.98×10^{10}	0.0	51000.0
87	$C_2H_5Cl \rightarrow C_2H_4 + HCl$	3.20×10^{13}	0.0	57600.0
	Class 8. Chain Termination Reactions			
88	$CH_2Cl + CH_2Cl \rightarrow CH_2ClCH_2Cl$	3.00×10^{38}	- 8.0	9431.0
89	$CH_2ClCHCl + Cl \rightarrow CHClCHCl + HCl$	1.00×10^{8}	2.0	0.0
90	$CHClCCl + Cl \rightarrow C_2Cl_2 + HCl$	1.00×10^{8}	2.0	3080.0
91	$CH_2Cl + CH_2Cl \rightarrow C_2H_3Cl + HCl$	1.10×10^{24}	- 3.2	8200.0
92	$CH_2ClCH_2 + Cl \rightarrow C_2H_3Cl + HCl$	1.10×10^{30}	- 4.7	17464.0
93	$C_2H_3 + Cl \rightarrow C_2H_2 + HCl$	4.70×10^{25}	- 3.2	11790.0
94	$C_2H_3 + CH_2Cl \rightarrow C_2H_2 + CH_3Cl$	1.00×10^{13}	0.0	0.0
95	$C_2H_3 + CH_2ClCHCl \rightarrow C_4H_5ClS + HCl$	1.98×10^{13}	0.0	7127.0
96	$C_2H_3 + CH_2ClCHCl \rightarrow C_4H_5ClU + HCl$	1.98×10^{13}	0.0	7127.0
97	$CH_2CCl + C_2H_3 \rightarrow C_4H_5ClS$	1.29×10^{12}	0.4	1565.0
98	$C_4H_5Cl_2S + Cl \rightarrow C_4H_4Cl_2 + HCl$	1.00×10^{7}	2.0	0.0
99	$C_4H_5Cl_2S + Cl \rightarrow C_4H_5ClS + Cl_2$	1.00×10^{7}	2.0	0.0
100	$C_4H_5Cl_2U + Cl \rightarrow C_4H_4Cl_2 + HCl$	1.00×10^{7}	2.0	0.0
101	$C_4H_5Cl_2U + Cl \rightarrow C_4H_5ClU + Cl_2$	1.00×10^{7}	2.0	0.0
102	$C_4H_5Cl_2S + CH_3 \rightarrow C_4H_5ClS + CH_3Cl$	1.00×10^{5}	2.0	0.0
103	$C_4H_6Cl + Cl \rightarrow C_4H_5ClS + HCl$	1.00×10^{7}	2.0	0.0
104	$C_4H_5U + Cl \rightarrow C_4H_4 + HCl$	1.00×10^{5}	2.0	0.0
105	$C_2H_5 + Cl \rightarrow C_2H_4 + HCl$	2.36×10^{23}	- 2.6	9735.0
106	$C_2H_3 + CH_2ClCHCl \rightarrow C_4H_6Cl_2$	1.21×10^{17}	- 1.2	3103.0
107	$CH_3CHCl + CH_2ClCHCl \rightarrow C_4H_6Cl_2 + HCl$	3.69×10^{13}	0.0	10689.0
108	$CH_2ClCH_2 + CH_2ClCHCl \rightarrow CH_2ClCH_2Cl + C_2H_3Cl$	1.00×10^{5}	2.0	0.0